UPPER BAY SURVEY

Final Report to the
Maryland Department of Natural Resources
Annapolis, Maryland 21401

VOLUME IV

Numerical Modeling

November 30, 1975

T. O. Munson
Project Chief Scientist

D. K. Ela
Project Manager

Carleton Rutledge, Jr.
Project Engineer and
Coordinating Editor

WESTINGHOUSE ELECTRIC CORPORATION
OCEANIC DIVISION
ANNAPOLIS, MARYLAND 21404

ABSTRACT

A numerical model has been developed to predict the source field from the concentration field of a passive contaminant subject to advection, diffusion, and settling velocity. The model is three-dimensional and is applied to the upper Chesapeake Bay.

The most realistic results have been obtained by using the model to predict the vertically integrated source function (the source of sediment per unit horizontal area per unit time).

The model was originally designed to predict the source field of sediment-borne chlorinated hydrocarbons (CHC) and polychlorinated biphenyls (PCB). The model finally was run as a predictor of suspended sediment sources only. Such a field, multiplied by a mean PCB and CHC concentration (per unit mass of sediment) does give one component of the PCB or CHC source field (i.e., the field that would result if the PCB or CHC concentration were constant in space) but not that component which is due to spatial variations in the PCB or CHC concentrations. Sufficient concentration data can be obtained in the future to achieve the original purpose of predicting the source field.

— —John R. Hunter

TABLE OF CONTENTS

LIST OF FIGURES

LIST OF TABLES

1. INTRODUCTION

John R. Hunter
Chesapeake Bay Institute
The Johns Hopkins University

A numerical model has been developed to predict the source field from the concentration field of a passive contaminant subject to advection, diffusion, and vertical settling velocity. The model is three-dimensional and, in this case, is applied to the upper Chesapeaker Bay. It can, however, be readily manipulated to cover any other body of water.

The complete model consists of ten discrete programs. The reasons for this segmentation are two-fold:

(1)   All the programs were designed to be run on computers of relatively low storage capacity (less than 20,000 numbers) such as the IBM 7094 at The Johns Hopkins University. For a three-dimensional model, this imposes a very stringent constraint, making multiple programs necessary.

(2)   Segmentation increases the versatility of the model as a whole. In the future, sections of the model may be readily modified in response to changes in input data quality and quantity, output requirements, and computer capabilities. Furthermore, certain aspects of the present modeling sequence are far from ideal. For example, an intrinsic requirement of a model of the transport processes of a contaminant in a fluid is the velocity field of that fluid. This could be derived from a quantity of current meter observations quite beyond the capabilities of the present study or a three-dimensional dynamic model of the water motions in the upper bay. Such a model does not exist at present; hence, a pseudo-dynamic model has been developed that predicts in a grossly simplified manner a *plausible* velocity field, based on observations of currents at the boundaries. This section of the total model, no doubt, can be replaced when present two and three-dimensional dynamic estuarine models have been adequately verified and developed into useable tools (e.g., the models of Leendertze et al., 1973, and Caponi, 1974).

2. THEORY

John R. Hunter
Chesapeake Bay Institute
The Johns Hopkins University

2.1 The Continuity Equations

The continuity equation for a passive contaminant subject to advection, diffusion, and a vertical settling velocity is:

$$\partial c/\partial t = \text{div } (\underset{\approx}{K} \text{ grad } c) - \text{div } (c(\underset{\sim}{u} + \underset{\sim}{u}_s)) + \sigma_1 \tag{1}$$

where c = concentration of contaminant/unit volume,

$\underset{\sim}{u}$ = fluid velocity vector,

$\underset{\sim}{u}_s$ = settling velocity vector (independent of position and time),

$\underset{\approx}{K}$ = a diffusivity tensor,

σ_1 = a source function for the contaminant, and

t = time coordinate.

The diffusivity tensor $\underset{\approx}{K}$ parameterizes the exchange processes for all motions of time scale less than the time scale used for averaging $\underset{\sim}{u}$ and c (e.g., Pritchard, 1958).

This equation would describe the transport properties of a sediment of concentration c and source function σ_1.

In the case of a sediment-borne contaminant, we assume the concentration of contaminant is a *conservative* property of the sediment. Hence, if α is the concentration of contaminant on the sediment (i.e., mass of contaminant/mass of sediment) and c is the concentration of sediment in the water, we may rewrite equation (1) by replacing c by αc and σ_1 by σ_2:

$$\partial/\partial t\, (\alpha c) = \text{div } (\underset{\approx}{K} \text{ grad } \alpha c) - \text{div } (\alpha c(\underset{\sim}{u} + \underset{\sim}{u}_s)) + \sigma_2. \tag{2}$$

This equation now describes the transport properties of a contaminant of concentration α per unit mass of sediment and source function σ_2. It is Equation (2) that we are to solve by numerical methods for the source σ_2 as a function of α, c, $\underset{\approx}{K}$, $\underset{\sim}{u}_s$, and $\underset{\sim}{u}$.

It is interesting to expand Equation (2):

$$\alpha \, \partial c/\partial t + c \, \partial \alpha/\partial t = \text{div}\,(\underset{\approx}{K}\,\alpha\,\text{grad}\,c + \underset{\approx}{K}\,c\,\text{grad}\,\alpha) - \alpha\,\text{div}\,c\,\underset{\sim}{u}$$

$$- c\,\underset{\sim}{u} \cdot \text{grad}\,\alpha - \alpha\underset{\sim}{u_s} \cdot \text{grad}\,c - c\,\underset{\sim}{u_s} \cdot \text{grad}\,\alpha + \sigma_2 \ (\text{using div}\,\underset{\sim}{u_s} = 0)$$

$$= \alpha\,\text{div}\,\underset{\approx}{K}\,\text{grad}\,c + \underset{\approx}{K}\,\text{grad}\,c \cdot \text{grad}\,\alpha$$

$$+ \text{div}\,(\underset{\approx}{K}\,c\,\text{grad}\,\alpha) - \alpha\,\text{div}\,c\underset{\sim}{u} - c\underset{\sim}{u} \cdot \text{grad}\,\alpha$$

$$- \alpha\,\underset{\sim}{u_s} \cdot \text{grad}\,c - c\,\underset{\sim}{u_s} \cdot \text{grad}\,\alpha + \sigma_2. \tag{3}$$

If we multiply Equation (1) by α:

$$\alpha\,\partial c/\partial t = \alpha\,\text{div}\,\underset{\approx}{K}\,\text{grad}\,c - \alpha\,\text{div}\,(c(\underset{\sim}{u} + \underset{\sim}{u_s})) + \alpha\,\sigma_1, \tag{4}$$

Subtracting Equation (4) from Equation (3):

$$c\,\partial \alpha/\partial t = (\underset{\approx}{K}\,\text{grad}\,c - c(\underset{\sim}{u} + \underset{\sim}{u_s})) \cdot \text{grad}\,\alpha + \text{div}(\underset{\approx}{K}\,c\,\text{grad}\,\alpha) + \sigma_2 - \alpha\,\sigma_1. \tag{5}$$

If we take the steady state case, $\partial \alpha/\partial t = 0$,

Re-arranging to give σ_2:

$$\sigma_2 = \alpha\sigma_1 + (\underset{\approx}{K}\,\text{grad}\,c - c(\underset{\sim}{u} + \underset{\sim}{u_s})) \cdot \text{grad}\,\alpha + \text{div}(\underset{\approx}{K}\,c\,\text{grad}\,\alpha). \tag{6}$$

There are thus two sources of contaminant:

(1) $\underline{\alpha\sigma_1}$:

This is simply the source of sediment scaled by the concentration of contaminant on that sediment. Such a source of contaminant can exist only where there is a source of sediment.

(2) The remainder of the right hand side of Equation (6):

This is probably the most important part of Equation (6), as it represents sources of contaminant *not necessarily associated with sources of sediment.* It is important to note that the terms depend on grad α, and thus our measurement of these sources of contaminant are critically dependent on our ability to measure accurately *variations* in α, and not simply an overall average value of α. If, within the limit of experimental error we find grad $\alpha = 0$, then Equation (6) becomes:

$$\sigma_2 = \alpha\,\sigma_1,$$

and modeling of the transport properties of the sediment-borne contaminant makes no contribution to our knowledge of σ_2.

2.2 A Note on Time-Averaging

Equation (2) contains variables that are understood to be averaged over a specific time period. This averaging is necessary to increase the confidence in the observed parameters, to remove short-term fluctuations that may have no relevance to future predictions, and to enable one to cope with a large body of data that was not taken synoptically. In this case, a suitable time period would appear to be of order a month. (In Section 3, time variations of the velocity field are discussed.) Hence, one should be able to predict *seasonal* changes in σ_2 but not *daily* changes. Changes over periods of time less than a month are either removed by this averaging (e.g., in linear terms such as $\partial/\partial t\,(\alpha c)$, σ_2) or are parameterized and included in the diffusion terms of Equation (2) (e.g., in non-linear terms such as div $(\alpha c\underset{\sim}{u})$). The diffusivity tensor $\underset{\approx}{K}$ hence must be understood as being the one applicable to a time-averaging period of the order of a month.

One probably is incapable of estimating $\partial/\partial t\,(\alpha c)$ to any degree of confidence and, hence, is forced to assume that $\partial/\partial t\,(\alpha c) = 0$. This assumption can be made more tenable by only considering periods when $\partial u/\partial t \simeq 0$ (i.e., times of maximum or minimum discharge from the Susquehanna River).

2.3 The Derivation of the Velocity Field

As described in Section 4, the numerical model consists of approximately 800 *boxes,* and 1200 interior *faces* where the horizontal water velocity must be known. (One may invoke the continuity equation for water to derive the vertical water velocities from the horizontal ones.) Also, from the current meter data described in Section 3, it is concluded that approximately 30 days of current observations are needed at each site to estimate a statistically significant mean velocity. Thus, it is inconceivable that sufficient velocity measurements could be made at all points in the model where such values are required. Some form of modeling of the velocity field is necessary to predict values at points in between *observational* points. Ultimately, the best solution probably is to use a three-dimensional dynamic model to predict the velocity field as a function of parameters defined at the boundaries of the body of water. Such a model is not currently available (See Section 1.); hence, a pseudo-dynamic model has been developed.

The general solution for the velocity field of a homogeneous body of water involves three dynamic and one kinematic equation to solve for the three components of velocity and pressure. For a non-homogeneous body of water, the additional variables introduced (density and the parameters on which density depends, e.g., salt, temperature) are accounted for by additional equations—an equation of state and the transport equations for the density-specifying parameters. In this case, one is interested only in the velocity field; hence, three equations are required to define it. The continuity equation for water serves as one. Another set of equations that would close the problem is to assume that the vorticity is everywhere zero:

$$\text{curl } \underset{\sim}{u} = 0. \tag{7}$$

(Due to the zero in the right hand side, this is only the equivalent of two equations; hence, the problem is not over-specified.) However, for an estuary where there is a significant vertical shear (or horizontal component of vorticity), a zero-vorticity assumption is clearly unrealistic. The approach taken is to derive a velocity field of *finite horizontal,* but *zero vertical* component of vorticity (a reasonable approximation in the estuarine case).

We apply transformation:

$$\underset{\sim}{u}' = \underset{\approx}{A}\,\underset{\sim}{u} \quad \text{(where } \underset{\approx}{A} \text{ is at present unspecified)} \tag{8}$$

and then assume:

$$\text{curl } \underset{\sim}{u}' = \text{curl } (\underset{\approx}{A}\underset{\sim}{u}) = 0. \tag{9}$$

Hence the *transformed* velocity field, $\underset{\sim}{u}'$, has zero vorticity, but Equation (9) does not necessarily imply that the *actual* vorticity (curl $\underset{\sim}{u}$) is zero.

Equation (9) implies that one can define a velocity potential, ϕ, for $\underset{\sim}{u}'$:

$$\underset{\sim}{u}' = -\text{grad } \phi; \tag{10}$$

Hence, Equation (8) becomes:

$$-\text{grad } \phi = \underset{\approx}{A}\,\underset{\sim}{u} \tag{11}$$

and inverting the matrix $\underset{\approx}{A}$:

$$u = -\underset{\approx}{A}^{-1}\,\text{grad } \phi. \tag{12}$$

If it is assumed the fluid is incompressible, and variations of parameters such as salt and heat do not affect the density significantly:

$$\text{div } \underset{\sim}{u} = 0. \tag{13}$$

Combining Equations (12) and (13):

$$\text{div} \, (\underset{\approx}{A}^{-1} \, \text{grad} \, \phi) = 0. \tag{14}$$

A sufficient boundary condition for Equation (14) is that the normal component of $(\underset{\approx}{A}^{-1} \, \text{grad} \, \phi)$ or $\underset{\sim}{u}$ be prescribed at all boundary faces.

From symmetry considerations, one principal axis of $\underset{\approx}{A}^{-1}$ will be considered vertical, the remaining two horizontal. We further assume that the two horizontal components are equal (i.e., there is no preferred horizontal direction). Hence if the (1) and (2) axes are horizontal and the (3) axis vertical:

$$\underset{\approx}{A}^{-1} = \begin{pmatrix} K_1 & 0 & 0 \\ 0 & K_1 & 0 \\ 0 & 0 & K_2 \end{pmatrix}.$$

$\underset{\approx}{A}^{-1}$ may be multiplied by any arbitrary constant, while Equation (14) remains unchanged. Hence, $K_1 = 1$ is chosen without any loss of generality; let $K_2 = K$:

$$\underset{\approx}{A}^{-1} = \begin{pmatrix} 1 & 0 & 0 \\ 0 & 1 & 0 \\ 0 & 0 & K \end{pmatrix}. \tag{15}$$

Equation (12) becomes:

$$\underset{\sim}{u} = -\underset{\sim}{i} \frac{\partial \phi}{\partial x} - \underset{\sim}{j} \frac{\partial \phi}{\partial y} - \underset{\sim}{k} \, K \frac{\partial \phi}{\partial z} \tag{16}$$

where x, y, z refer to the (1), (2), (3) axes, respectively, and $\underset{\sim}{i}, \underset{\sim}{j}, \underset{\sim}{k}$ are the respective unit vectors. Equation (14) becomes:

$$\text{div} \left(\underset{\sim}{i} \frac{\partial \phi}{\partial x} + \underset{\sim}{j} \frac{\partial \phi}{\partial y} + \underset{\sim}{k} \, K \frac{\partial \phi}{\partial z} \right) = 0,$$

$$\text{or} \quad \frac{\partial^2 \phi}{\partial x^2} + \frac{\partial^2 \phi}{\partial y^2} + K \frac{\partial^2 \phi}{\partial z^2} = 0 \tag{17}$$

(Equation (17) is simply Laplace's equation if a new z-coordinate given by $z/\sqrt{K}$ is chosen.)

The vorticity of this velocity field is given by:

$$\underset{\sim}{\zeta} = - \, \text{curl} \, (\underset{\approx}{A}^{-1} \, \text{grad} \, \phi), \tag{18}$$

which in our case is:

$$\underset{\sim}{\zeta} = (1\text{-}K) \left(\underset{\sim}{i} \frac{\partial^2 \phi}{\partial y \partial z} - \underset{\sim}{j} \frac{\partial^2 \phi}{\partial x \partial z} \right) \tag{19}$$

Hence, there is no *vertical* component of vorticity, but horizontal components exist if $K \neq 1$. Equation (18) may be written:

$$\underset{\sim}{\zeta} = \underset{\sim}{L} \, \phi, \tag{20}$$

where L is the linear vector operator:

$$(- \, \text{curl} \, \underset{\approx}{A}^{-1} \, \text{grad}).$$

Any component of $\underset{\sim}{\zeta}$ may be denoted by ζ_i where

$$\zeta_i = L_i \, \phi,$$

(21)

where L_i is the $_i$th component of $\underset{\sim}{L}$.

Now, div $(\underset{\approx}{A}^{-1}$ grad $\zeta_i) = $ div $(\underset{\approx}{A}^{-1}$ grad $(L_i\phi))$

and, since L_i is a scalar operator containing only derivatives and constant, this becomes:

L_i (div$(\underset{\approx}{A}^{-1}$ grad $\phi)) = L_i$ (0) from Equation (14)

$$= 0.$$

Hence, $\qquad\qquad$ div $(A^{-1}$ grad $\zeta_i) = 0,$

(22)

and any component of $\underset{\sim}{\zeta}$ obeys the same equation as ϕ (This is independent of any assumptions made about $\underset{\approx}{A}^{-1}$ other than it is constant.)

The three principal components of $\underset{\approx}{A}^{-1}$ may be thought of as diffusion coefficients governing the distribution of $\underset{\sim}{\zeta}$ as a function of the values of $\underset{\sim}{\zeta}$ prescribed at the boundaries. (The component of $\underset{\sim}{\zeta}$ parallel to a vertical boundary face may be prescribed by the vertical shear of the horizontal velocity normal to that face using Equation (19)).

A solution of Equation (22) is:

$$\zeta_i = \zeta_0 \, e^{\,(k_x x + k_y y + k_z z)} ,$$

(23)

where k_x, k_y, k_z are constants,

$$\text{and } k_x^2 + k_y^2 + K k_z^2 = 0$$

(24)

If we look at the two-dimensional case, neglecting y-variations, and let $k_z = j\pi/d$ where $j^2 = -1$:

from Equation (23): $\qquad\qquad \zeta_i = \zeta_o \, e^{k_x x} \, e^{j \frac{\pi z}{d}} ,$

(25)

from Equation (24): $\qquad\qquad k_x^2 = \frac{K\pi^2}{d^2}$

(26)

This may be considered to represent diffusion of vorticity in the x-direction from a vertical boundary, at $x = 0$, at which the vorticity profile is given by a cosine function, with zeros at $z = \pm d/2$. If these are taken to be the upper and lower boundaries of a body of fluid, one may investigate how far the vorticity can diffuse horizontally into the fluid.

At the origin, the vorticity is given by $\zeta_i = \zeta_o$. The vorticity at $z = 0$ falls to 1/e of this value at $x = -1/k_x = \pm \, d/\pi \sqrt{K}$.

Hence to model an estuarine circulation where a two-layered flow exists to a distance of order L from the seaward boundary, one must define a suitable vorticity at the boundary (by defining a suitable vertical shear in the horizontal velocity), and choose K from:

$$L = d/\pi \sqrt{K} ,$$

or $K = d^2/\pi^2 L^2$, where d is the water depth.

(27)

For the model of the upper Chesapeake Bay, $d \sim 500$ cm, $L \sim 2.5 \times 10^6$ cm and hence:

$$K = 4 \times 10^{-9}.$$

The velocity field thus is derived by solution of Equation (14), with the normal components of $\underset{\sim}{u}$ defined at all external boundaries.

Equation (14) was solved by the method of successive over-relaxation.

2.4 The Derivation of the Exchange Coefficient Field

The exchange coefficient field is derived from observations of the concentration of a passive contaminant which has zero settling velocity and zero source distribution. Hence for this contaminant (in this case salinity is used) Equation (1) reduces to:

$$\partial c/\partial t = \text{div} \ (\underset{\approx}{K} \ \text{grad} \ c) - \text{div} \ (\underset{\sim}{cu}). \tag{28}$$

Equations (1) and (28) hold strictly for c given as concentration *per unit volume*. However, it can be shown easily that, by an assumption of incompressibility and the Boussinesq approximation, the equations also hold if c is understood to be concentration *per unit mass* of fluid as in the case of salinity.

Taking the averaging period for c and u to be of order a month and taking $\partial c/\partial t = 0$ by considering times of maximum or minimum discharge from the Susquehanna River (Section 2.2),

Equation (28) becomes:

$$\text{div} \ (\underset{\approx}{K} \ \text{grad} \ c) = \text{div} \ (\underset{\sim}{cu}). \tag{29}$$

If the field of c and u were known, one still would not know the field of $\underset{\approx}{K}$ uniquely. Hence, one must make further assumptions about $\underset{\approx}{K}$. As will be shown in Section 4, one assumes $\underset{\approx}{K}$ is of the form:

$$\underset{\approx}{K} = \begin{pmatrix} K_H & 0 & 0 \\ 0 & K_H & 0 \\ 0 & 0 & K_V \end{pmatrix}$$

where, as before, axes (1) and (2) are horizontal and (3) is vertical.

K_H is the horizontal diffusivity and is a function of x and y only.

K_V is the vertical diffusivity and is a function x, y, and z.

If the boundary conditions are properly posed, these assumptions and Equation (29) are sufficient for the derivation of the $\underset{\approx}{K}$ field.

A knowledge of the fields of c (the salinity) and u are required. The field of $\underset{\sim}{u}$ is derived as in Section 2.3. The field of c is obtained from all the historical data collected in the upper Chesapeake Bay during the relevant season. (The model is applied to spring and fall conditions.) However, these observations are far from complete, and an interpolation procedure is necessary to generate the complete field. As will be shown, it is important that this procedure is chosen carefully. Two possibilities are suggested:

2.4.1 Solution of $\nabla^2 c = 0$ Over All Points Other Than Those Where c is Specified By Observations

In one dimension, this is equivalent to linear interpolation between known values, and Equation (29) reduces to:

$$\frac{\partial}{\partial x} (K \frac{\partial c}{\partial x}) = \frac{\partial}{\partial x} (cu) ,$$

or $\quad K = \dfrac{cu + c_o}{\dfrac{\partial c}{\partial x}} \quad$ where c_o is a constant, and K is a scalar diffusivity.

At a point where c is specified by observations, there will be in general a discontinuity in $\partial c/\partial x$, hence, a discontinuity in K. Similarly in two or three dimensions, there exist discontinuities in grad c at *observation* points. $\underset{\approx}{K}$ grad c is continuous, as a discontinuity in $\underset{\approx}{K}$ grad c would lead to a singularity in div ($\underset{\approx}{K}$ grad c), which we know we do not have in div (cu)(by Equation (29). However, the discontinuity in grad c would again lead to a discontinuity in $\underset{\approx}{K}$. *This is not considered desirable.*

2.4.2 Solution Of $\nabla^4 c = 0$ Over All Points Other Than Those Where c is Specified By Observations.

In one dimension this is:

$$\partial^4 c/\partial x^4 = 0.$$

Integrating:

$$c = a_0 + a_1 x + a_2 x^2 + a_3 x^3.$$

The procedure thus is a cubic spline with matching of the second and lower derivatives at *observation* points. $\partial c/\partial x$ varies continuously everywhere, so K also varies continuously. In two or more dimensions $\nabla^2 c$, grad c, and c are continuous; hence, by a similar argument used in Section 2.4.1, K is continuous also. *We thus chose this interpolation method.*

However, in an estuarine situation where the vertical scales are in the order of 10^{-4} times the horizontal scales, the procedure $\nabla^4 c = 0$ will cause an interpolated point to be drastically over-weighted with respect to points on the same vertical line, and under-weighted with respect to points on the same horizontal plane. We hence transform the z-coordinate by:

$$z \text{ new} = z \text{ old}/\sqrt{K} \qquad \text{and then solve } \nabla^4 c = 0.$$

(This is equivalent to re-defining the operator ∇^2 as $(\partial^2/\partial x^2 + \partial^2/\partial y^2 + K \partial^2/\partial z^2)$ in the untransformed coordinates.)

In this case, choose $K = 10^{-6}$.

Assume that at the boundaries the normal gradients of c and $\nabla^2 c$ are zero.

The solution $\nabla^4 c = 0$ is obtained by the method of successive over-relaxation.

Having derived complete fields of $\underset{\sim}{u}$ and c, there remains the solution of Equation (29) for $\underset{\approx}{K}$. As $\underset{\approx}{K}$ is a function of position and hence included *within* the divergence term on the left hand side of Equation (29), $\underset{\approx}{K}$ can be solved only by inversion of a large matrix containing functions of $\underset{\sim}{u}$ and c. Inversion of this matrix by relaxation is not possible as the solution would not converge. Hence a gradient method is used for the required inversion.

2.5 An Alternative Method of Estimating the Exchange Coefficients.

As will be shown in Section 4.5, the exchange coefficients derived from the historical salinity data, by the method of Section 2.4.2, showed considerable *noise* and did not yield satisfactory results for the source field of suspended sediment. This was probably due to the noise inherent in the salinity data, which was taken over many different years. Another approach for determining the exchange coefficients was hence required.

The method chosen was to specify that (1) the horizontal exchange coefficient was independent of direction and position, and (2) the vertical exchange coefficient was independent of position. The optimum values of these two scalar variables were then derived by minimizing, in a least-squares sense, the suspended sediment source predictions for all *boxes* not adjacent to the lateral or bottom boundaries of the bay. Neglecting any sources of sediment due to *fallout* onto the sea surface and also neglecting organic production in the water column, then in reality the source function for each of these boxes should be zero.

If the horizontal diffusivity is denoted by K_H and the vertical by K_V, then it can easily be shown that the source function for any box is given by:

$$\sigma = c_1 K_H + c_2 K_v + c_3,$$

where c_1, c_2, and c_3 are functions of the concentration field.

Hence, summing over all boxes not adjacent to the lateral or bottom boundaries, the source *sum of squares* is:

$$SS = \Sigma \sigma^2 = a_1 K_H^2 + a_2 K_v^2 + a_3 K_H K_v + a_4 K_H + a_5 K_v + a_6,$$

where $a_1, \ldots, a_6$ are functions of the concentration field.

Using six estimations of SS for different values of K_H and K_v, the values of $a_1, \ldots, a_6$ may be derived and hence the values of K_H and K_v to give a *minimum* in SS. These are the *optimum* values of K_H and K_v.

In the case of the upper Chesapeake Bay sediment data, it was found that the optimum K_H turned out to be small and negative. As this was not realistic, a further constraint was applied, that $K_H = 0$.

2.6 Derivation of Concentration Field Of Sediment-Borne Contaminant.

One ultimately wishes to solve Equation (2) for the source field of contaminant. This requires a knowledge of the field of αc, while our observations of αc (as with salinity) are far from complete. To generate the required field, we use the same procedure as used for salinity, described in Section 2.4.2.

2.7 Derivation Of The Source Field Of Sediment-Borne Contaminant.

This follows directly from Equation (2), using a steady state assumption (Section 2.2):

$$\sigma_2 = -\text{div} \left(\underset{\approx}{K} \, \text{grad} \, (\alpha c) \right) + \text{div} \left(\alpha \, c \, (\underset{\sim}{u} + \underset{\sim}{u}_s) \right). \tag{30}$$

From a knowledge of the fields of $\underset{\approx}{K}$, αc, $\underset{\sim}{u}$, and $\underset{\sim}{u}_s$, the field of σ_2 is derived explicitly by finite difference methods.

3. CURRENT VELOCITY OBSERVATIONS

John R. Hunter
Chesapeake Bay Institute
The Johns Hopkins University

Current measurements taken under Contracts DACW31-70-C-0078 and DACW31-70-C-0077 for the U. S. Army Corps of Engineers (Klepper, 1972) and measurements taken as part of the present project were used as indicators of the mean velocity field in the upper Chesapeake Bay. Unfortunately the data are not ideal for the reasons discussed below.

3.1 Duration of Data.

The bulk of data for the Corps of Engineers contract was taken in July, August, and October 1971. One set of data for the present contract was taken in April 1974, the other in October 1974. Ideally, it is best to model the maximum flow (spring) and minimum flow (fall) conditions. The data for spring (during which time the bulk of sediment probably enters the bay) are thus solely confined to one 11-day period in April 1974 and to only two cross-sections of the bay, representing estimates of the mean velocity vector at only 14 points in space.

Further, as shown later in this section, due to large oscillations of periods approximately two days and longer in the tidally filtered current velocities, the durations of current observations are really inadequate to provide much confidence that calculated means are representative of long-term means. (The measurement periods are: six or seven days for the Corps of Engineers data, 11 days for the April 1974 data, and ten days for the October 1974 data.)

3.2 Quality of Data

Serious doubts must be cast on the observations of surface velocity obtained for the Corps of Engineers contract. These were taken with Savonius-rotor current meters in the severely wave-contaminated zone at depths of only two or four feet. As far as mean velocities are concerned, these measurements are probably worthless.

Further, in most cases, the bottom current meter was only about three feet from the bottom, essentially in the bottom boundary layer. Hence these measurements tell little about what is happening in the water column above the boundary layer. Of 21 current meter stations, 17 contain three current meters or less, two meters of which (the surface and bottom) gave data of little value. The remaining current meter (if it exists) tells nothing of the vertical variation in velocity. Of the remaining four stations, one is in the Chester River and one in the Patapsco River, neither of which is particularly important in determining the velocity field of the model. The remaining two stations (CB-07-03, CB-07-05) are in the northern part of the model and are of no use for boundary values.

As an example of the low confidence that one can place in mean velocities obtained from this data, Figure 1 shows a comparison of the velocity profiles obtained at Stations CB-07-03 and CB-07-04 over the same period (July 23 through 30, 1971) at a position approximately 76°12'W, 39°20'N. The stations were only 950 meters apart (the width of the bay at this point is about 5,000 meters). As mentioned above, Station CB-07-03 is one of the only two stations where we could hope to obtain information about the velocity profile.
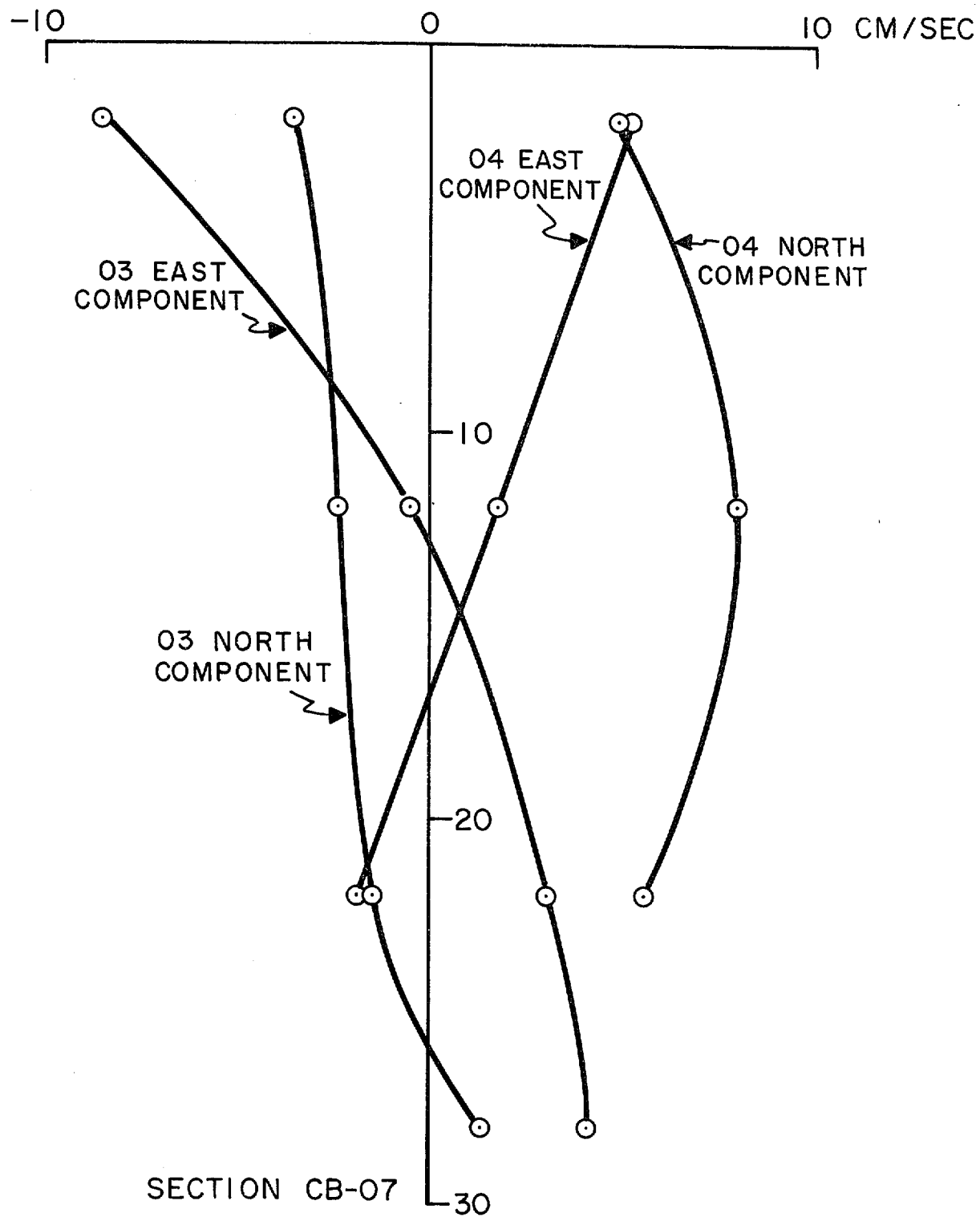
Figure 1. Velocity Profiles at Stations CB-07-03 And CB-07-04 Over The Period
July 23 - 30, 1971

75151A401

3.3 Methods of Measurement

The data collected for the Corps of Engineers are described by Klepper (1972).

The data collected for the present contract were taken with Braincon-1381 and Endeco-105 current meters. The sampling interval was 10 to 20 minutes for the Braincon meters and 30 minutes for the Endeco meters. The mooring system was essentially as described by Klepper (1972), except:

(a)   Plank-on-edge buoys were not used.

(b)   Surface buoyancy was obtained either by using a styrofoam float or a decked-in fiberglass dinghy.

(c)   Where possible, near-surface measurements were taken using Endeco meters, which are of the propeller type and less susceptible to wave contamination.

3.4 Method of Analysis

The observed current vectors were converted to components in directions true east and true north. These components were then filtered for the removal of the tides, using a numerical filter due to Cartwright (see references). The filter chosen was low pass, with the response shown in Figure 2. The response is in the range zero to -0.01 for all diurnal constituents of periods less than 26.7 hours and is 0.0008 for the M2 constituent. The span of time covered by the filter multipliers is 80 hours; hence, 40 hours of data are lost at each end of the record when the filter is applied. The resultant velocity components indicate non-tidal variations. To derive an estimate of the longterm mean, the filtered components are averaged over the new record length. The effect of this is the same as taking an average over the original record, using a weighting function that is constant except for tapers over the first and last 80 hours of the record. These tapers cause the final mean to be virtually independent of the tides.

The reading errors (due to the resolution of the recording mechanism) for current velocity are of order ±1 cm/sec for the meters used. The number of observations in a record were in the order of 1,000; hence, if one assumes the reading errors are independent, the error in the mean due to reading errors is of order:

$$\pm 1/\sqrt{1,000}\ \text{cm/sec} \sim \pm 0.03\ \text{cm/sec}.$$

However the reading errors are dependent to a certain extent, and some error cancellation will occur giving an accuracy of better than this. More important are probably random errors due to the compass direction reading and systematic errors due to wave contamination, misalignment of the meter in the flow, compass calibration errors, and velocity calibration errors. The latter is probably negligible, while the others are little understood. A reasonable guess is that possibly the error is dominated by a systematic direction error of order five or ten degrees, and in the case of a Savonius rotor meter, a wave contamination error in the order of 1 cm/sec. The direction error would give an error in the order of 1 cm/ sec in one of the components of a 10 cm/sec mean current.

However, as will be shown from the data collected in April and October 1974, there is a standard deviation in the order of 3 cm/sec in each record of the filtered current velocity components, primarily due to oscillations of periods approximately two days and longer. The error in our estimate of the longterm mean is therefore probably dominated by this large current variability (which is regarded as real) rather than in instrumental errors.

3.5 Results

The tidally filtered velocity components, meaned over the record lengths, are given in Tables 1 and 2 for the Corps of Engineers data and for the data collected for the Upper Bay Survey.

As an estimate of the variability of the tidally filtered components, the span of values of each filtered record is tabulated in Table 3 together with the mean filtered values from Table 2 for the 1974 data. The span is defined as the maximum value in the filtered record less the minimum value in the filtered record.
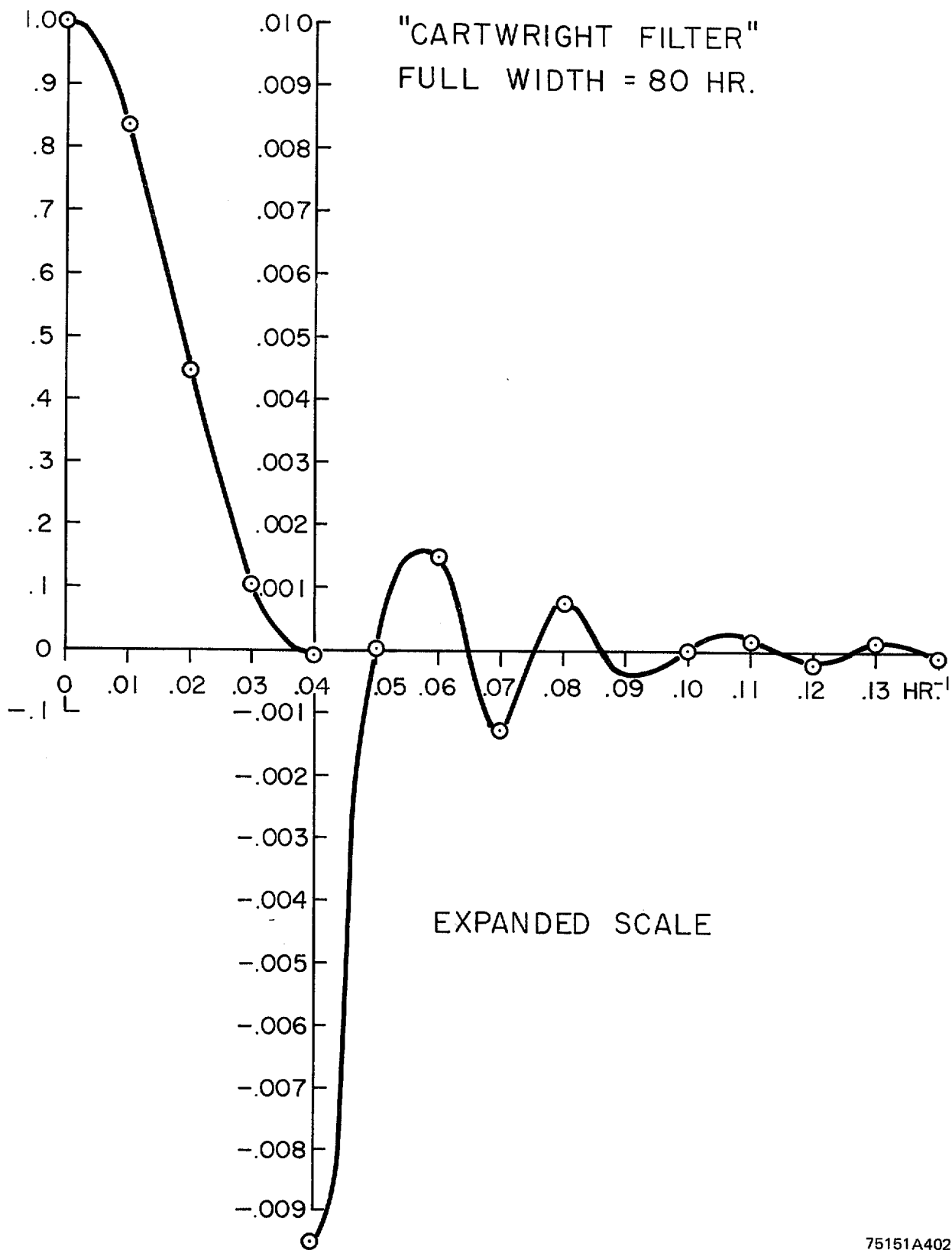
Figure 2. Response From Application of Cartwright's Numerical Filter (Full Width is 80 Hours)

75151A402

TABLE 1. TIDALLY FILTERED VELOCITY COMPONENTS FROM CORPS OF ENGINEERS DATA

STATION	POSITION						DEPTH	DURATION OF DATA		EAST COMPONENT (cm/sec)	NORTH COMPONENT (cm/sec)
	Latitude			Longitude				Start	Finish		
	Deg.	Min.	Sec.	Deg.	Min.	Sec.	(Ft.)				
E 01 01	39	26	35	75	59	41	4	10/4/71	10/10/71	−0.59	−3.86
E 01 01							12	10/4/71	10/10/71	−0.12	−3.11
E 01 01							18	10/4/71	10/10/71	0.81	−4.57
SA 01 01	39	22	32	76	02	21	4	10/5/71	10/10/71	−2.38	3.53
BN 0101	39	14	36	76	24	56	4	8/3/71	8/8/71	2.40	−0.03
GR 01 01	39	18	28	76	18	49	2	8/3/71	8/4/71	Record Too Short	
GR 01 01							12	8/3/71	8/9/71	−1.95	0.02
GR 01 01							20	8/3/71	8/9/71	−0.36	1.02
MR 01 01	39	17	27	76	23	10	4	8/2/71	8/9/71	−4.21	−2.61
MR 01 01							8	8/2/71	8/9/71	−2.74	0.51
MA 01 01	39	03	25	76	26	14	4	10/5/71	10/12/71	1.04	−3.62
MA 01 01							12	10/5/71	10/12/71	−3.20	1.98
MA 01 01							18	10/5/71	10/12/71	−5.39	1.92
CH 01 01	39	00	43	76	11	04	4	10/11/71	10/18/71	2.94	−4.61
CH 01 01							12	10/11/71	10/18/71	2.38	−1.33
CH 01 01							22	10/11/71	10/18/71	1.24	−0.06
CH 01 01							32	10/11/71	10/18/71	−0.62	1.33
CH 01 01							42	10/11/71	10/18/71	−3.15	2.83
CH 01 01							52	10/11/71	10/17/71	−4.43	5.29
BR 01 01	39	20	30	76	14	39	4	7/23/71	7/30/71	2.27	2.48
BR 01 01							8	7/23/71	7/30/71	−5.86	3.19

TABLE 1. TIDALLY FILTERED VELOCITY COMPONENTS FROM CORPS OF ENGINEERS DATA (Continued)

STATION	POSITION						DEPTH	DURATION OF DATA		EAST COMPONENT (cm/sec)	NORTH COMPONENT (cm/sec)
	Latitude			Longitude				Start	Finish		
	Deg.	Min.	Sec.	Deg.	Min.	Sec.	(Ft.)				
PR 01 01	39	09	21	76	26	35	2	8/3/71	8/9/71	−0.89	−9.13
PR 01 01							14	8/3/71	8/9/71	3.43	−2.09
PR 01 02	39	10	22	76	26	34	2	8/3/71	8/9/71	0.22	−12.62
PR 01 02							13	8/3/71	8/9/71	4.72	−5.27
PR 01 03	39	10	45	76	26	33	2	8/3/71	8/9/71	−3.09	−9.40
PR 01 03							12	8/3/71	8/9/71	1.16	−3.24
PR 01 03							22	8/3/71	8/9/71	0.84	1.10
PR 01 03							32	8/3/71	8/9/71	−2.67	1.61
PR 01 03							38	8/3/71	8/9/71	−2.46	1.89
CB 06 01	39	08	08	76	23	42	2	7/23/71	7/30/71	3.22	1.91
CB 06 01							12	7/23/71	7/30/71	−2.16	−0.42
CB 06 01							20	7/23/71	7/25/71	Record Too Short	
CB 06 02	39	08	21	76	21	13	2	7/23/71	7/30/71	−4.61	−1.13
CB 06 02							12	7/23/71	7/30/71	−2.75	−2.02
CB 06 02							18	7/23/71	7/30/71	−1.74	−0.62
CB 06 03	39	08	27	76	20	07	2	7/23/71	7/30/71	−3.86	0.67
CB 06 03							22	7/23/71	7/30/71	−9.59	5.02
CB 06 03							32	7/23/71	7/30/71	3.77	3.30
CB 06 04	39	08	20	76	19	23	2	7/23/71	7/28/71	5.96	5.90
CB 06 04							22	7/23/71	7/30/71	−7.99	4.62
CB 06 04							32	7/23/71	7/30/71	4.70	1.95

TABLE 1. TIDALLY FILTERED VELOCITY COMPONENTS FROM CORPS OF ENGINEERS DATA (Continued)

STATION	POSITION						DEPTH	DURATION OF DATA		EAST COMPONENT (cm/sec)	NORTH COMPONENT (cm/sec)
	Latitude			Longitude				Start	Finish		
	Deg.	Min.	Sec.	Deg.	Min.	Sec.	(Ft.)				
CB 06 05	39	08	39	76	18	37	2	7/23/71	7/30/71	−7.06	2.49
CB 06 05							12	7/23/71	7/30/71	−10.85	1.86
CB 07 01	39	20	42	76	12	53	4	7/23/71	7/30/71	−0.30	2.48
CB 07 01							11	7/23/71	7/30/71	2.48	1.98
CB 07 02	39	20	13	76	12	20	2	7/23/71	7/30/71	−23.50	4.67
CB 07 02							13	7/23/71	7/30/71	−2.71	−7.70
CB 07 03	39	19	57	76	12	02	2	7/23/71	7/30/71	−8.62	−3.61
CB 07 03							12	7/23/71	7/30/71	−0.50	−2.42
CB 07 03							22	7/23/71	7/30/71	3.03	−1.48
CB 07 03							28	7/23/71	7/30/71	4.18	1.25
CB 07 04	39	19	33	76	11	37	2	7/23/71	7/30/71	5.06	4.83
CB 07 04							12	7/23/71	7/30/71	1.77	7.89
CB 07 04							22	7/23/71	7/30'71	−1.82	5.59
CB 07 05	39	19	22	76	11	24	2	7/23/71	7/30/71	−3.02	1.49
CB 07 05							12	7/23/71	7/30/71	−0.99	0.17
CB 07 05							22	7/23/71	7/30/71	0.78	−0.09
CB 07 05							32	7/23/71	7/30/71	1.26	1.27

TABLE 2. TIDALLY FILTERED VELOCITY COMPONENTS FROM UPPER BAY SURVEY DATA

STATION	POSITION						DEPTH	DURATION OF DATA		EAST COMPONENT (cm/sec)	NORTH COMPONENT (cm/sec)
	Latitude			Longitude				Start	Finish		
	Deg.	Min.	Sec.	Deg.	Min.	Sec.	(Ft.)				
S 1	39	23	49	76	02	53	4	4/15/74	4/26/74	−7.99	−10.12
S 1							12	4/15/74	4/26/74	−4.13	−9.69
S 1							22	4/15/74	4/26/74	−10.12	−9.37
S 2	39	24	38	76	04	06	4	4/15/74	4/17/74	Record Too Short	
S 2							10	4/15/74	4/17/74	Record Too Short	
S 3	39	25	24	76	05	15	4	4/15/74	4/17/74	Poor Data	
S 3							10	4/15/74	4/26/74	−3.93	0.96
T 1	39	12	55	76	14	55	4	4/15/74	4/26/74	−7.39	−12.97
T 1							12	4/15/74	4/23/74	−6.20	−9.06
T 1							22			No Data	
T 1							32	4/15/74	4/26/74	3.03	10.77
T 1							42	4/15/74	4/26/74	2.03	17.40
T 2	39	13	32	76	17	04	4	4/15/74	4/26/74	−5.99	−3.42
T 2							10	4/15/74	4/26/74	−2.47	−3.32
T 3	39	14	16	76	19	36	4	4/15/74	4/22/74	−0.98	1.95
T 3							10	4/15/74	4/26/74	−3.39	−0.20
T 3							15	4/15/74	4/26/74	−5.42	0.51
T 4	39	14	52	76	21	33	4	4/15/74	4/26/74	−3.16	1.98
T 4							10	4/15/74	4/26/74	Data Not Reduced	

TABLE 2. TIDALLY FILTERED VELOCITY COMPONENTS FROM UPPER BAY SURVEY DATA (Continued)

STATION	POSITION						DEPTH	DURATION OF DATA		EAST COMPONENT (cm/sec)	NORTH COMPONENT (cm/sec)
	Latitude			Longitude				Start	Finish		
	Deg.	Min.	Sec.	Deg.	Min.	Sec.	(Ft.)				
SS 1	39	02	30	76	23	30	6			No Data	
SS 1							15	10/10/74	10/17/74	−0.14	−2.18
SS 1							24	10/07/74	10/17/74	2.95	−1.42
SS 1							33			No Data	
SS 2	39	02	30	76	21	30	7			No Data	
SS 2							15	10/07/74	10/17/74	−2.50	3.89
SS 2							24	10/07/74	10/17/74	−0.03	4.06
SS 2							33	10/07/74	10/17/74	0.23	−0.02
SS 3	39	02	30	76	19	30	4			No Data	
SS 3							12	10/07/74	10/17/74	−2.28	2.36
SS 4	39	02	30	76	16	30	5			No Data	
SS 4							15			No Data	
SS 4							25	10/07/74	10/17/74	−4.26	−6.57
T 1	39	12	55	76	14	55	5	10/07/74	10/17/74	−0.59	−1.69
T 1							15			No Data	
T 1							25	10/07/74	10/17/74	0.77	10.10
T 1							35	10/07/74	10/17/74	2.58	14.50
T 1							45	10/07/74	10/17/74	2.62	13.75
T 2	39	13	32	76	17	04	7	10/07/74	10/12/74	−2.50	−5.64
T 3	39	14	16	76	19	36	3	10/07/74	10/17/74	0.76	−1.53
T 3							13	10/07/74	10/17/74	−3.18	6.27
T 4	39	14	52	76	21	33	7			Data Not Reduced	

TABLE 3. VARIABILITY OF THE TIDALLY FILTERED COMPONENTS

STATION	DEPTH (Ft)	PERIOD	EAST COMPONENT		NORTH COMPONENT	
			MEAN (cm/sec)	SPAN (cm/sec)	MEAN (cm/sec)	SPAN (cm/sec)
S 1	4	April 1974	−7.99	9.50	−10.12	12.39
S 1	12	April 1974	−4.13	4.16	−9.69	7.00
S 1	22	April 1974	−10.12	7.76	−9.37	10.33
S 3	10	April 1974	−3.93	8.48	0.96	4.66
T 1	4	April 1974	−7.39	13.77	−12.97	16.89
T 1	12	April 1974	−6.20	7.25	−9.06	16.87
T 1	32	April 1974	3.03	5.87	10.77	31.08
T 1	42	April 1974	2.03	3.24	17.40	22.40
T 2	4	April 1974	−5.99	9.61	−3.42	19.55
T 2	10	April 1974	−2.47	7.18	−3.32	11.31
T 3	4	April 1974	−0.98	6.11	1.95	5.22
T 3	10	April 1974	−3.39	9.41	−0.20	6.65
T 3	15	April 1974	−5.42	11.83	0.51	5.11
T 4	4	April 1974	−3.16	3.62	1.98	7.01
SS 1	15	Oct 1974	−0.14	7.28	−2.18	13.43
SS 1	24	Oct 1974	2.95	11.40	−1.42	6.05
SS 2	15	Oct 1974	−2.50	5.07	3.89	24.58
SS 2	24	Oct 1974	−0.03	10.47	4.06	18.91
SS 2	33	Oct 1974	0.23	9.12	−0.02	10.59
SS 3	12	Oct 1974	−2.28	4.65	2.36	2.09
SS 4	25	Oct 1974	−4.26	7.64	−6.57	13.20
T 1	5	Oct 1974	−0.59	11.41	−1.69	17.08
T 1	15	Oct 1974	0.77	3.83	10.10	19.63
T 1	35	Oct 1974	2.58	3.84	14.50	22.96
T 1	45	Oct 1974	2.62	2.54	13.75	17.73
T 2	7	Oct 1974	−2.50	3.30	−5.64	2.32
T 3	3	Oct 1974	0.76	6.58	−1.53	7.46
T 3	13	Oct 1974	−3.18	8.93	6.27	5.89

The spans are approximately 7 cm/sec for the east component and 13 cm/sec for the north component, for both the April and October data. The corresponding moduli of mean filtered values are of order 5 cm/sec, 7 cm/sec, 2 cm/sec, and 5 cm/sec for the April east, April north, October east, and October north sets of data respectively. The span of values is always greater than the mean, and in some cases it is as much as twice the mean. The standard deviations of the filtered values may be estimated from:

Standard deviation ~0.35 span (for a sinusoid).

The source of this variability is in general due to oscillations of period approximately two days and longer in the filtered values. Figure 3 shows results for the most and least variable stations in April 1974 (Stations T1 and S1), and Figure 4 shows the results for the most and least variable stations in October 1974 (Stations T1 and SS3). Also plotted is the discharge of the Susquehanna River at Conowingo for these periods. All velocity plots show evidence of oscillations of a two-day period and longer. The Conowingo discharge also shows considerable variation over the duration of the measurements.

By inspection of Tables 1 and 2, it is seen that many stations do not seem estuarine at all- -the water appears to flow landward at the surface and seaward at the bottom. As a simple analysis of this, each station was given a score as follows:

Denoting the near-surface north component by u_s and the near-bottom north component by u_b:

Score +1 if $u_s < u_b$

Score −1 if $u_s > u_b$

Score zero if there is only one meter in the water column.

These scores are shown in Table 4, the totals indicating that a large number of stations show no estuarine character at all. It is suggested that: (1) this is because the durations of the current meter experiments were too short, and (2) the mean filtered velocities obtained are not representative of a longterm mean.

3.5.1 Conclusions

As mentioned in Section 2.2, it was necessary to make a steady state assumption in the continuity equation for the sediment-borne contaminant. The interpolation procedure described in Section 2.3 is suitable only for steady state velocity fields. In deriving the exchange coefficient field according to Section 2.4, it was necessary to use salinity data that was taken from many different years and was distributed through the spring and fall seasons. From these considerations, it is imperative to aim at estimating longterm mean values of parameters for use in our model. In this context, *longterm* defines a period in the order of a month (i.e., sufficiently short that seasonal changes are unimportant), and such mean values should be consistent from year to year.

Month-long records of current velocities in the upper bay are not available. The longest continuous records are for 11 days only. Station CB-07-03 covers a 16-day period in July and August with a four-day gap in the middle, and a 14-day period in October with a change of current meters in the middle of the period. Time has not permitted either of these records to be analyzed as a whole. Hence, there is no data for estimating the importance of time scales of periods longer than about ten days.

There are strong indications of two-day periods and longer (e.g., the April 1974 data in Figure 2), which show a periodicity in the order of six days, and the October 1974 data at Station T1 show a definite trend. The Conowingo discharges also show strong variations over the measurement period. In April 1974, the flow showed a trend, changing in value by a factor of two over the record. In October 1974, when admittedly the discharge was small and probably not as important in determining the estuarine dynamics, the flow varied by an order of magnitude over the record.
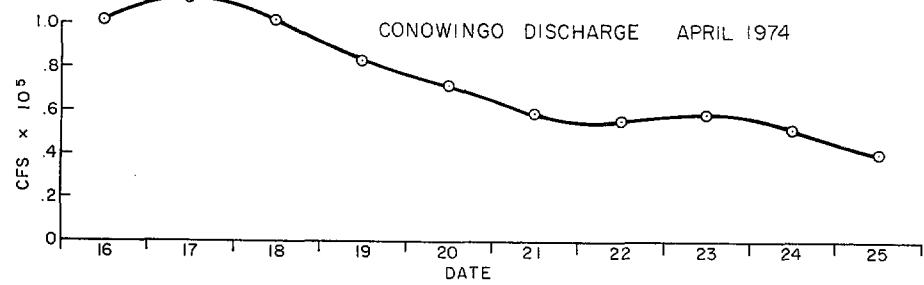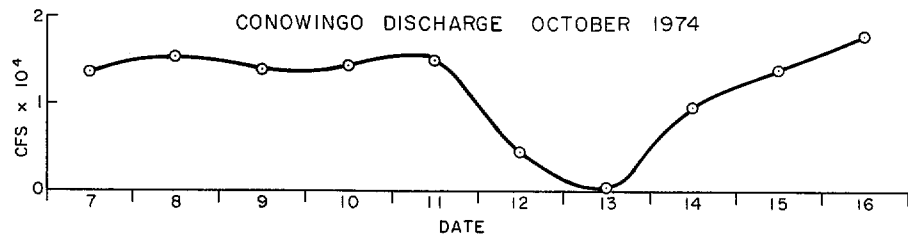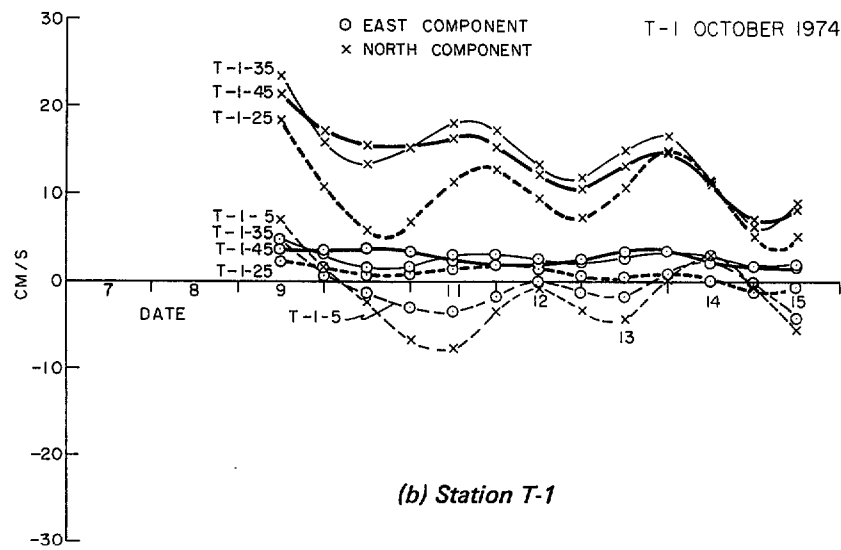
(a) Conowingo Discharge
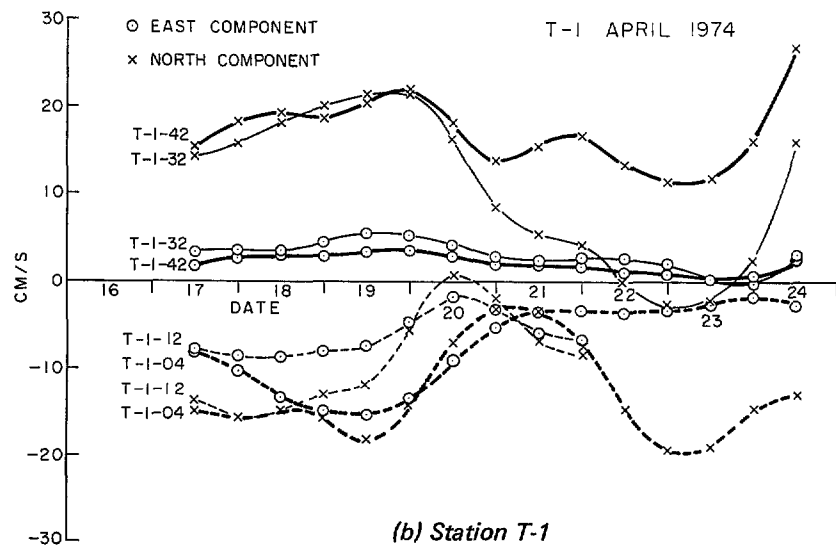
(b) Station T-1
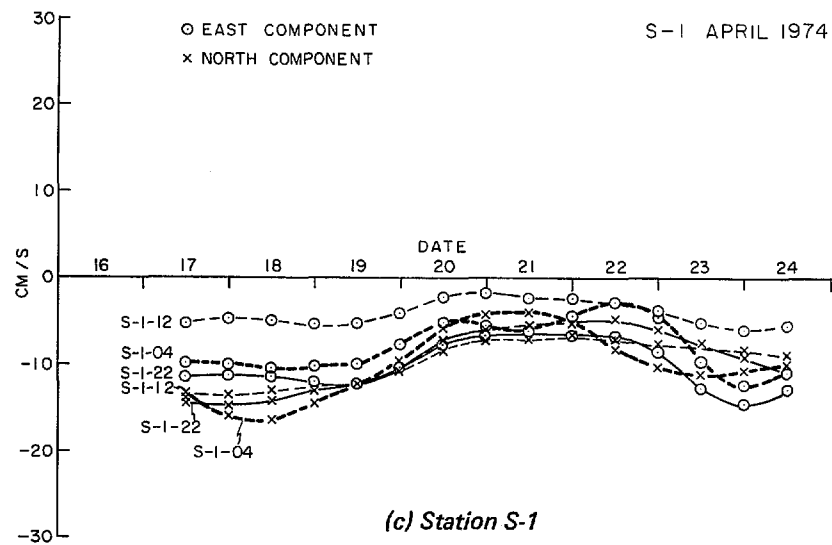
(c) Station S-1
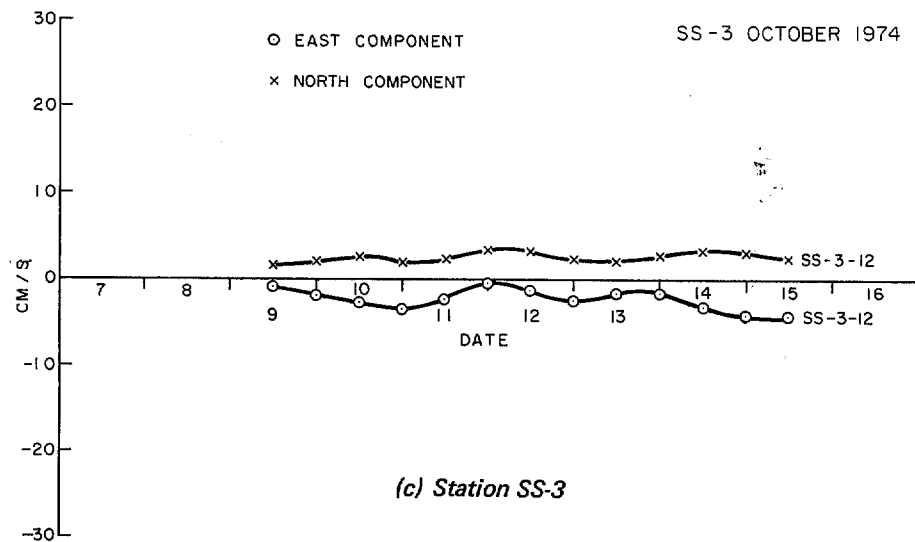
75151A403

Figure 3. Results, April 1974

3-12

(a) Conowingo Discharge

(b) Station T-1

(c) Station SS-3

75151A404

Figure 4. Results, October 1974

TABLE 4. ESTUARINE SCORES
(Stations on Upper Bay — Cross-Sections Only)

STATION	SCORE
CB 06 01	−1
CB 06 02	+1
CB 06 03	+1
CB 06 04	−1
CB 06 05	−1
CB 07 01	−1
CB 07 02	−1
CB 07 03	+1
CB 07 04	+1
CB 07 05	−1
S 1	+1
S 3	0
T 1 (April 1974)	+1
T 2 (April 1974)	+1
T 3 (April 1974)	−1
T 4 (April 1974)	0
SS 1	+1
SS 2	−1
SS 3	0
SS 4	0
T 1 (Oct. 1974)	+1
T 2 (Oct. 1974)	0
T 3 (Oct. 1974)	+1

TOTALS: 10 x (+1)

                8 x (−1)

                5 x (0)

TOTAL SCORE = +2

MAXIMUM POSSIBLE SCORE = +23

Therefore, the data on hand are not satisfactory for determining with confidence the longterm mean. It is suggested that a measurement period in the order of 30 days would be necessary for this determination. It is necessary, therefore, to make various assumptions about the flow pattern from discharge data at Conowingo and from judicious inspection of the current meter profiles on hand. The best longterm estimates are the Conowingo discharge data that are discussed below.

3.5.2 Conowingo Discharge

Two different estimates of the Susquehanna River flow at Conowingo are available:

(1) The natural river flow, which is the Susquehanna's flow if the dam at Conowingo were absent, and

(2) The total discharge, which is the measured discharge through the dam at Conowingo. If one requires the flow of water into the upper Chesapeake Bay then it is the total discharge that is the relevant parameter.

However, Boicourt (1969) computed the average monthly *natural river flows* at Conowingo for the period 1929-1966, and it would seem sensible to use these values if they are a good approximation to the total discharge. Data were available for the period 1961-1966 for monthly values of *both* natural river flow *and* total discharge. Hence, one is able to estimate the agreement between the two parameters as described below.

The root mean square (rms) difference between the two monthly estimates for the period 1961-1966 was:

0.4×10^3 cubic feet per second (cfs),
while the mean discharge over this period was:
27.4×10^3 cfs.

Dividing these values to give the proportion rms difference in the estimates gives 0.015 or 1.5 percent.

Hence using *natural river flow* instead of *total discharge* would give an error of only about 1.5 percent and hence is regarded as acceptable. As will be shown later, this error is much less than the difference between the data for 1974 and the longterm mean data.

Also from Boicourt (1969) (Figure 5), the *high flow* period was chosen as being represented by March and April, and the *low flow* being represented by July to October. These periods henceforth will be referred to as the *high flow* and *low flow* periods, and they will serve as the basis for two distinct runs of the numerical model programs.

One may investigate how representative of the longterm mean was 1974, the year of our observations:

From Boicourt's data, the *natural river flow*, averaged over the period 1929-1966 and over the months March and April, was:

80,788 cfs.
For March and April 1974, the mean total discharge was:
73,455 cfs.

These differ by 9.1 percent; hence, the 1.5 percent error in equating *natural river flow* with *total discharge* is negligible. It is concluded that March and April 1974 were reasonably representative of the longterm mean conditions.

Again from Boicourt's data, *natural river flow*, averaged over the period 1929-1966 and over the months July-October, was:

11,837 cfs.
For July-October 1974, the *total discharge* was:
15,354 cfs.

CONOWINGO NATURAL RIVER FLOW
ENSEMBLE AVERAGE BY MONTH
1929—1966
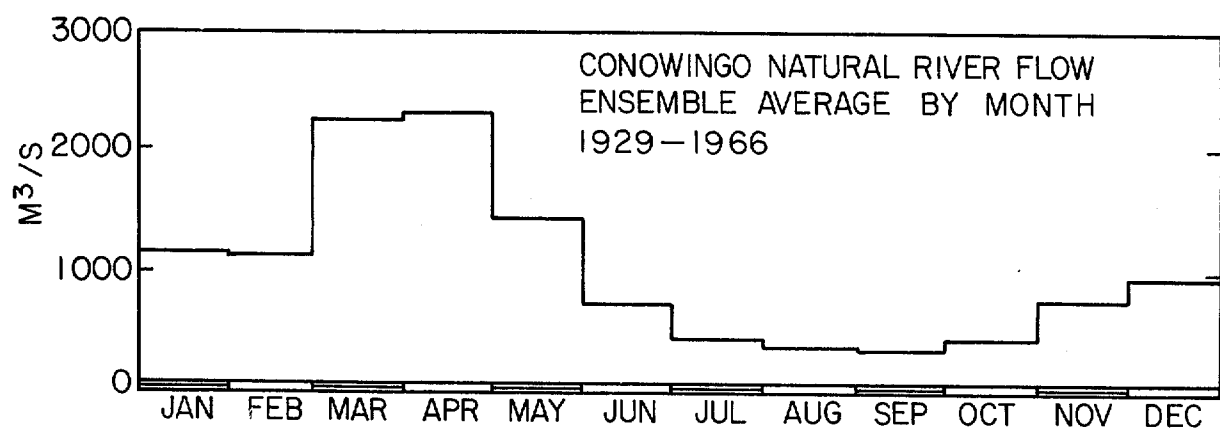
75151A405

Figure 5. Conowingo Natural River Flow, Ensemble Average by Month, 1929-1966

These differ by 29.7 percent, and again the 1.5 percent error in equating natural river flow with total discharge is negligible.

The agreement between the 1974 value and the longterm mean is not as good as for March and April, but if one takes the *absolute differences* instead of the *proportional differences*:

For March and April the difference was:
7,333 cfs.
For July-October the difference was:
3,517 cfs.

Hence on an *absolute scale*, the agreement for July-October was better than for March and April. It is concluded that July-October 1974 was a period also reasonably representative of the longterm mean conditions.

Since the velocity field data are being used in conjunction with *historical records* of salinity from the Chesapeake Bay Institute data bank, it was elected to model the *longterm mean* contaminant distributions and not specifically the *1974* distributions. Therefore, it is assumed that the 1974 field measurements were representative of longterm mean conditions. Also the longterm mean flow estimates of Boicourt (covering the period 1929-1966) are used as input to the numerical model.

Hence, from Boicourt's data, the following flows at Conowingo were chosen:

March-April	(High Flow):	80,788 cfs, or
		2,288 cubic meters per second (m³/s)
July-October	(Low Flow):	11,837 cfs, or
		335.2 m³/s.

3.5.3 Use of Drainage Area Statistics

Flow data for all the lateral boundaries of the upper Chesapeake Bay are required as input to the velocity field prediction model. This is deduced in our case using the drainage area statistics for the region (Seitz, 1971). The assumptions are made that (1) evaporation approximately equals precipitation over water areas and (2) the flow of water at any section of a river or of the upper bay is proportional to the total land drainage area above that section. Seitz's data includes land drainage areas for sections every five miles up all the rivers entering the upper Chesapeake Bay, for east-west sections across the upper bay at every five minutes of latitude, and for Conowingo (Table 5). Also on the table is a column headed *deficit* which is the extra drainage area for each five-minute segment of the upper bay that is not accounted by the drainage areas of all the listed rivers flowing into that segment.

Hence if: F_N = drainage area for northern section of 5' segment,
F_S = drainage area for southern section of 5' segment, and
R_i = drainage area for i^{th} river flowing into the segment,

(31)

then the *deficit*, $D = F_S - F_N - \sum_i R_i$,

where $\sum$ denotes summation over all rivers for that segment.

The drainage areas are divided by the drainage area for the southernmost section (39°00') and given in the next column of the table. These will be denoted by the primed quantities:

F_N', F_S', R_i', and D'.

The deficits are rather difficult to deal with in the velocity field prediction model, which for reasons of economy relies on inflow data specified at rivers entering the upper Chesapeake Bay only. Hence the deficit is included as drainage area assigned to the rivers by multiplying the area for each river of a specific bay segment by a constant.

Equation (31) may be divided by the drainage area for the (39°00') section and rearranged.

TABLE 5. LAND DRAINAGE AREA STATISTICS
(After Seitz, 1971)

SECTION (As per Seitz, 1971)	AREA (Square Statute Miles)	DEFICIT (Square Statute Miles)	AREA (Area For 39° 00')	CORRECTED PROPORTIONAL AREAS
CONOWINGO	27089.00		0.9114293	0.9114293
39° 30'	27595.82		0.9284816	0.9284816
E ϕ	233.69	39.91	0.0078627	0.0092055
39° 25'	27869.42		0.9376871	0.9376871
SF ϕ	84.94	59.98	0.0028579	0.0036619
BUR ϕ	128.26		0.0043154	0.0055294
39° 20'	28142.60		0.9468784	0.9468784
G ϕ	448.62		0.0150941	0.0163394
M ϕ	9.92	42.65	0.0003338	0.0003613
B ϕ	58.41		0.0019652	0.0021273
39° 15'	28702.20		0.9657066	0.9657066
PA ϕ	552.05	6.25	0.0185741	0.0187844
39° 10'	29260.50		0.9844910	0.9844910
CH 10	399.91	1.52	0.0134553	0.0142685
39° 05'	29684.58		0.9987595	0.9987595
MA ϕ	30.36	6.51	0.0010215	0.0012405
39° 00'	29721.45		1.0000000	1.0000000

$$F'_S = F'_N + \sum_i R'_i + D'$$

$$= F'_N + (1 + \frac{D'}{\sum_i R'_i}) \sum_i R'_i$$

$$= F'_N + \sum_i (1 + \frac{D'}{\sum_i R'_i}) R'_i.$$

Hence,
$$F'_S = F'_N + \sum_i R''_i , \qquad\qquad (32)$$

where
$$R''_i = (1 + \frac{D'}{\sum_i R'_i}) R'_i$$

Hence Equation (32) is satisfied without the necessity of a deficit. The corrected river drainage areas (R''_i) are given in the next column of Table 5 with those for the east-west bay sections and Conowingo (which do not have to be corrected).

If the corrected drainage area for any section is denoted by S, that for Conowingo by C, and the flow at Conowingo by J_c, then the flow at the section is given by:

$$J_c S/C.$$

3.5.4 Velocity Profiles

For all lateral boundaries except the southern boundary, a uniform flow across the river sections was chosen.

For the southern boundary, the flow is divided into two components:

(1) The *mean flow*, uniform across the section, and derived from the Conowingo flow and drainage area statistics as in Section 3.5.3.

(2) A *stratified flow* of zero mean over the section that approximates as closely as possible the flow as measured by current meters. From the current meter observations, the depth of the layer of no motion was estimated and was used as depth of no motion for this stratified flow. (Addition of a mean flow to the stratified flow will change this depth of no motion slightly, but this change is not very large.)

4. DETAILS OF THE MODEL.

John R. Hunter
Chesapeake Bay Institute
The Johns Hopkins University

4.1 Finite Difference Mesh

As the model was to be three-dimensional, a rectilinear finite difference mesh was chosen, rather than the common *box model* approach in which each *box* may be of a different volume and shape. To simplify data input, the mesh points were chosen to coincide horizontally with those of the Chesapeake Bay Institute data bank (Feister and Karweit, 1973), giving a mesh size of one minute of latitude by one minute of longitude. The vertical mesh spacing was chosen to give two mesh points, on average, from the surface to the bottom. The average depth of the upper Chesapeake Bay relative to mean low water is 11.0 feet (using depths read from C&GS Charts 1225 and 1226). The vertical mesh spacing was thus chosen as 5.0 ft. The upper surface of the model was taken to be mean low water. The lateral and bottom boundaries of the model were chosen by calculating the mean depth of water (read from C&GS Charts 1225 and 1226) for the rectangle, of sides one minute latitude and one minute longitude, surrounding each mesh point. Areas of land were taken to have zero depth. The mean depth in feet, for each rectangle was then divided by five and rounded to the nearest integer. The resultant value gave the number of mesh points vertically from the surface to the bottom for that particular rectangle. Where the resultant value was zero, the rectangle was considered outside the model.

The arrangement of mesh points and parameters defined at each mesh point is shown schematically in Figure 6 for the case of a water depth of three mesh spacings or 15 feet. The *box* and *face* notation is helpful in identifying *mesh points*; each *box point* (shown by a circle) may be considered the center of a cuboid (the box) and each *face point* (shown by a cross) thus lies at the center of a *box face*. The lateral, surface, and bottom boundaries of the model consist of a series of *face points*. K_x and K_y (to be defined more rigorously later) are interpolations of K_H values onto the face points. And u, v, and w are the components of the water velocity vector, $\underset{\sim}{u}$.

The lateral boundaries of the model of the upper Chesapeake Bay are shown in Figure 7. Mesh points are defined by integers I, J, and K. If the mesh spacings are denoted by δx, δy, and δz for the three respective axes, then the coordinates of the box point (I, J, K) are:
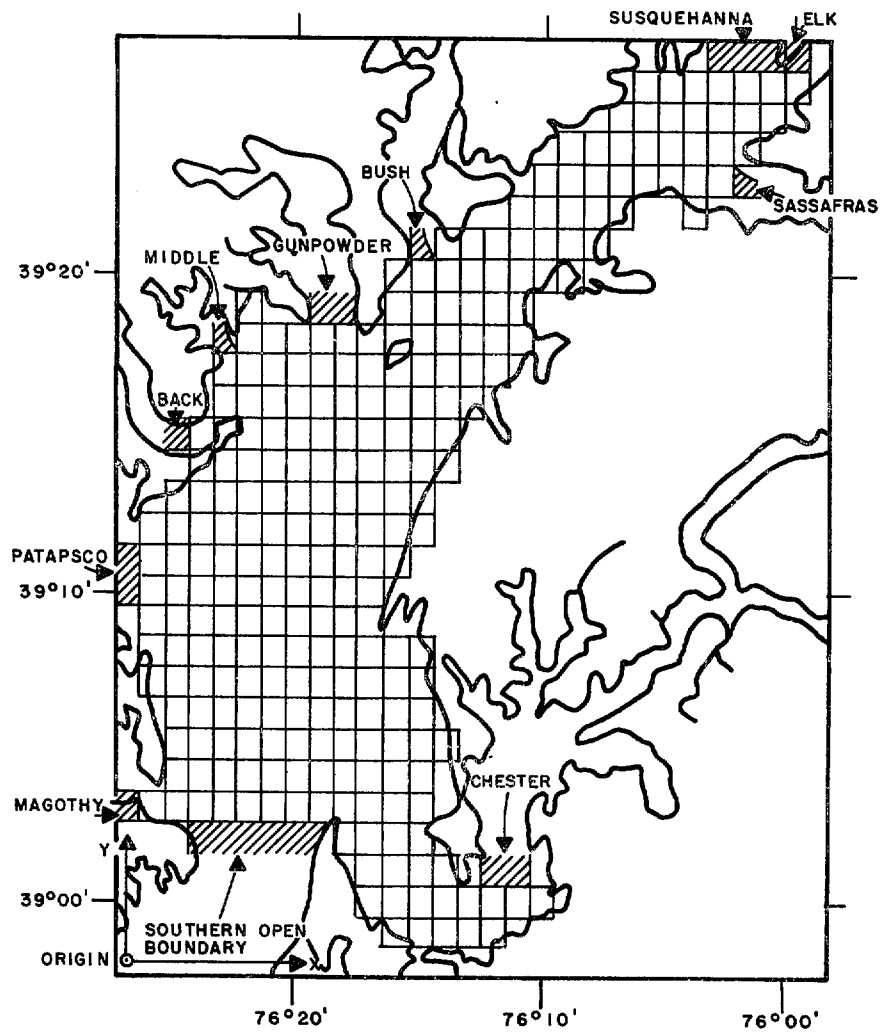
$$I\delta x, \quad J\delta y, \quad K\delta z$$

In this case, δx = 1' arc of longitude
δy = 1' arc of latitude
δz = 5 ft.
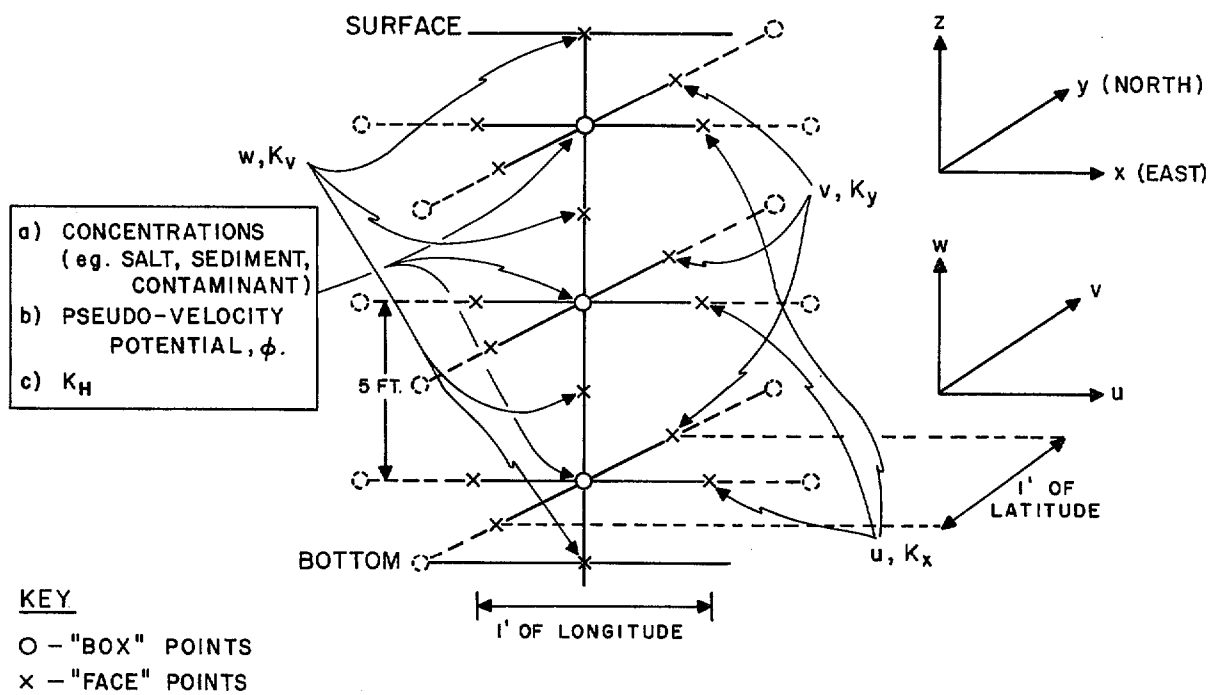
Figure 6. Arrangement of Mesh Points and the Parameters at Each Mesh Point

75151A406

Figure 7. Lateral Boundaries of the Model of the Upper Chesapeake Bay

75151A407

Face points fall in between box points; hence, if the same convention is used as for box points, non-integer values of I, J, or K would have to be used. Hence, the following convention is used for face points:

A face denoted by I, J, K lies at:

$(I - 1/2) \delta x$, $J\delta y$, $K\delta z$ for a face with a normal parallel to the x-axis,

$I\delta x$, $(J - 1/2) \delta y$, $K\delta z$ for a face with a normal parallel to the y-axis,

$I\delta x$, $J\delta y$, $(K - 1/2) \delta z$ for a face with a normal parallel to the z axis.

The horizontal position of the origin is shown in Figure 7.

The vertical position of the origin is 10.5 mesh spacings or 52.5 ft below mean low water. Hence, the top surface of the model (taken as mean low water) is given by the face points denoted by (I, J, 11). The highest box points (2.5 ft below mean low water) are denoted by (I, J, 10).

Frequently a parameter is specified at a point of one type (e.g., box or face), and its value is required at a point of the other type. In these cases *linear interpolation* between adjacent points is used to derive the new value.

The upper Chesapeake Bay model consists of 799 box points. As a check on the method used to define the model boundaries, the volume of the model was compared with that of Boicourt (1969):

Volume present model $= 2,057 \times 10^6 \mathrm{m}^3$
Volume Boicourt's model $= 2,033 \times 10^6 \mathrm{m}^3$,

representing a difference of only 1.2 percent.

Also shown in Figure 7 are the various tributaries to the upper bay, the flows through which are determined by the Conowingo flow and by drainage area statistics (Section 3.5.3).

4.2 Velocity Field Determination

As described in Section 3.5.3, the *mean flow* through the upper bay and its tributaries is defined by the Conowingo flow and drainage area statistics. In addition to this, a *stratified flow* of zero mean is specified at the sourthern boundary. The depth of no motion was taken to be about 20 ft for both the high and low cases. The stratified flows that best fit the current observations are shown in Figure 8. The section shown is the southern boundary of the model; velocities are in centimeters per second (cm/sec) and are positive towards the north.
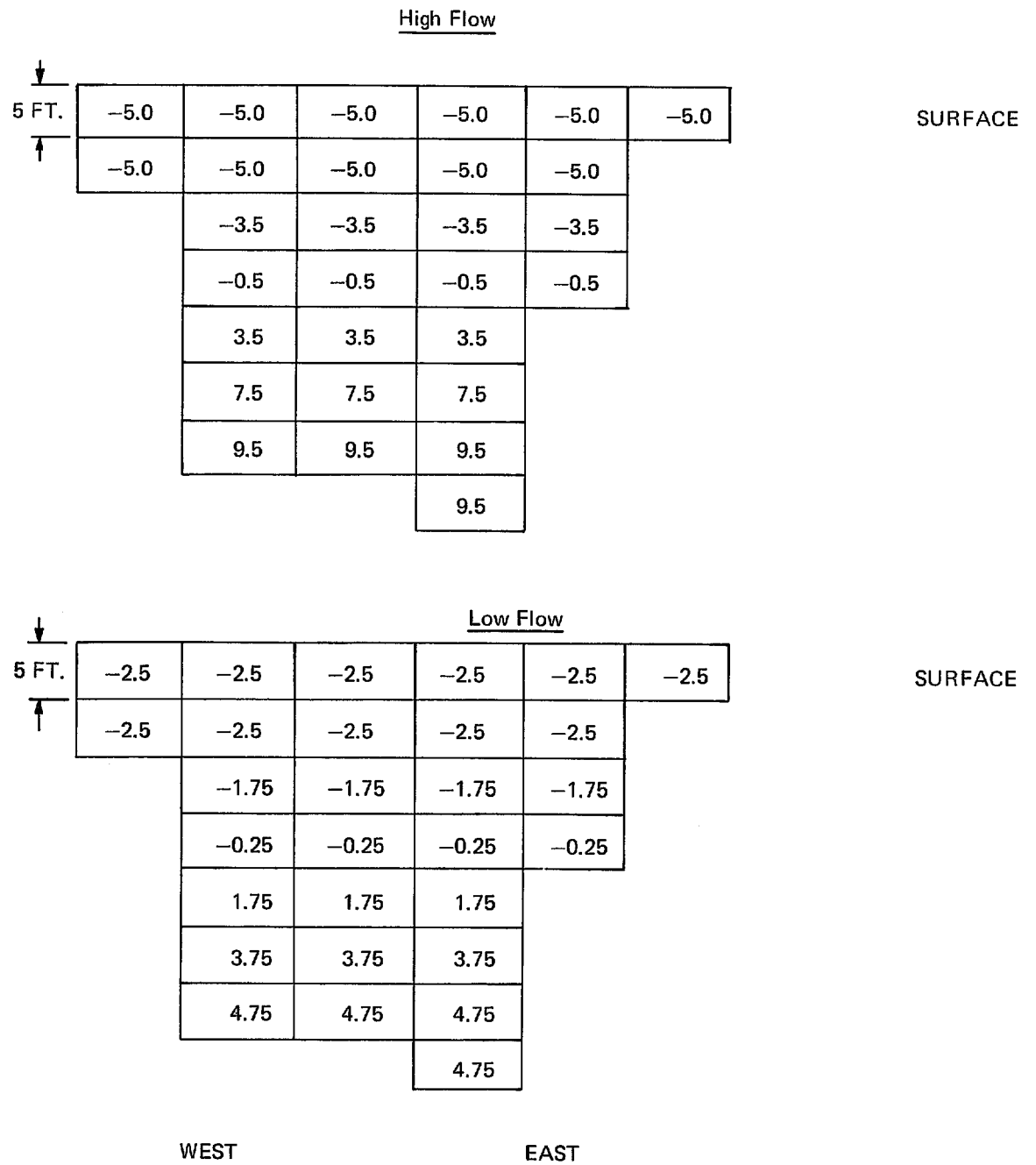
These velocities were fed into the model described in Section 2.3 as boundary conditions, and a solution to Equation (14) was found by successive over-relaxation.

The resultant velocity fields for levels K = 8 and K = 10 under high and low flow conditions are shown in Figures 9 through 12.

4.3 Exchange Coefficient Determination

It can be shown that if the concentration field of a conservative contaminant (in this case salt) and the velocity field are known, then the exchange coefficient field can be obtained if we impose the following conditions:

(1)   The contaminant concentration is specified at box points.
(2)   The velocity components are specified at face points as shown in Figure 6.
(3)   The vertical exchange coefficient is specified at all face points where w is specified, and it is a function of depth.
(4)   The horizontal exchange coefficient is independent of direction in a horizontal plane, is independent of depth, and is specified at box point (This is denoted by "K_H" in Figure 6). In any prediction model using these exchange coefficients, values interpolated onto face points are required. These are denoted by K_x and K_y in Figure 6.

High Flow

High Flow

5 FT.	−5.0	−5.0	−5.0	−5.0	−5.0	−5.0	SURFACE
	−5.0	−5.0	−5.0	−5.0	−5.0		
		−3.5	−3.5	−3.5	−3.5		
		−0.5	−0.5	−0.5	−0.5		
		3.5	3.5	3.5			
		7.5	7.5	7.5			
		9.5	9.5	9.5			
				9.5			

Low Flow

5 FT.	−2.5	−2.5	−2.5	−2.5	−2.5	−2.5	SURFACE
	−2.5	−2.5	−2.5	−2.5	−2.5		
		−1.75	−1.75	−1.75	−1.75		
		−0.25	−0.25	−0.25	−0.25		
		1.75	1.75	1.75			
		3.75	3.75	3.75			
		4.75	4.75	4.75			
				4.75			

WEST   EAST

75151A408

Figure 8. Stratified Flows Best Fitting the Current Observations

4-5

HIGH FLOW

50 CM/S

K = 8
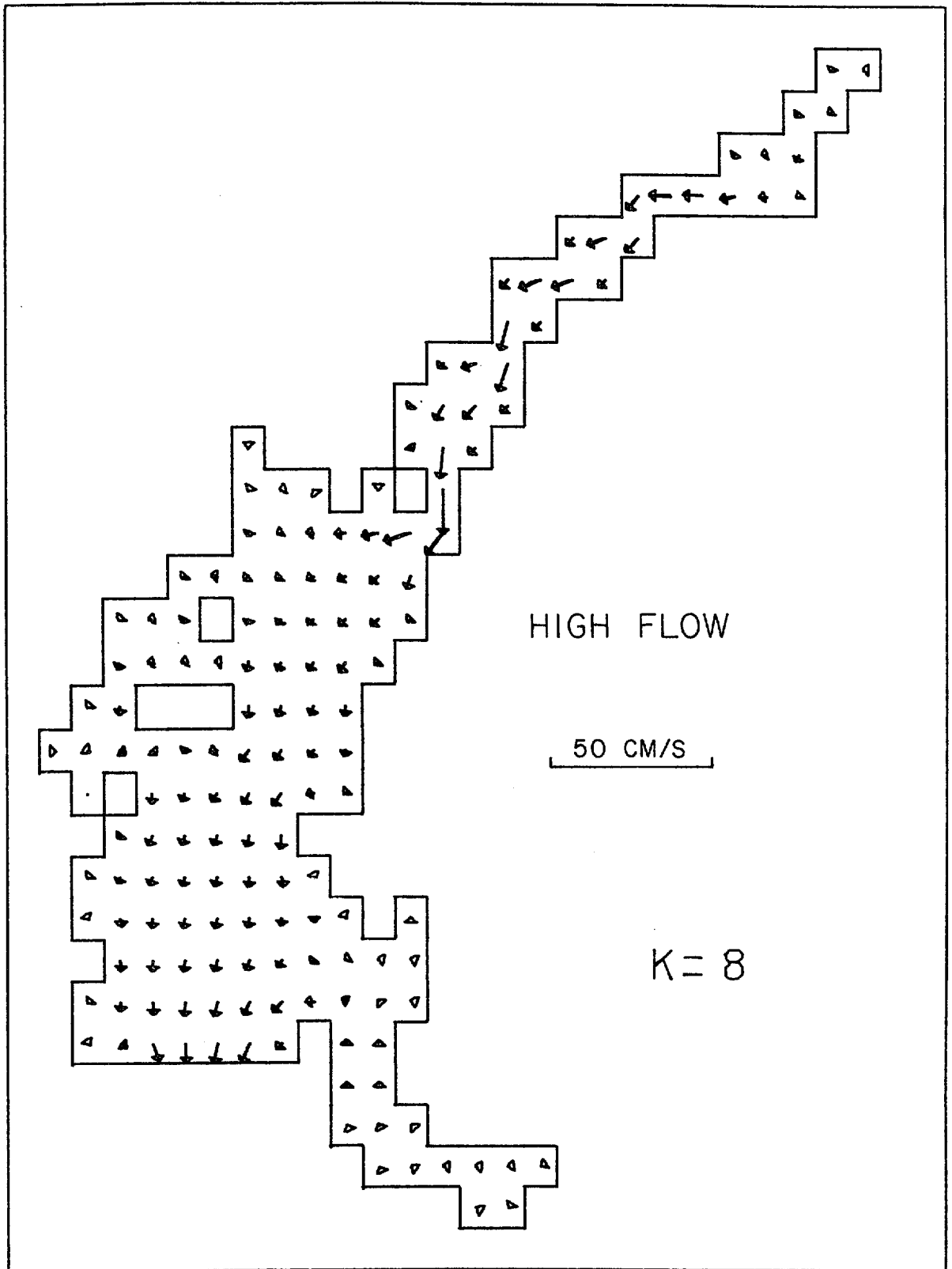
75151A409

Figure 9. Resultant Velocity Field for Level K = 8 Under High Flow Conditions

4-6

HIGH FLOW

50 CM/S

K = 10
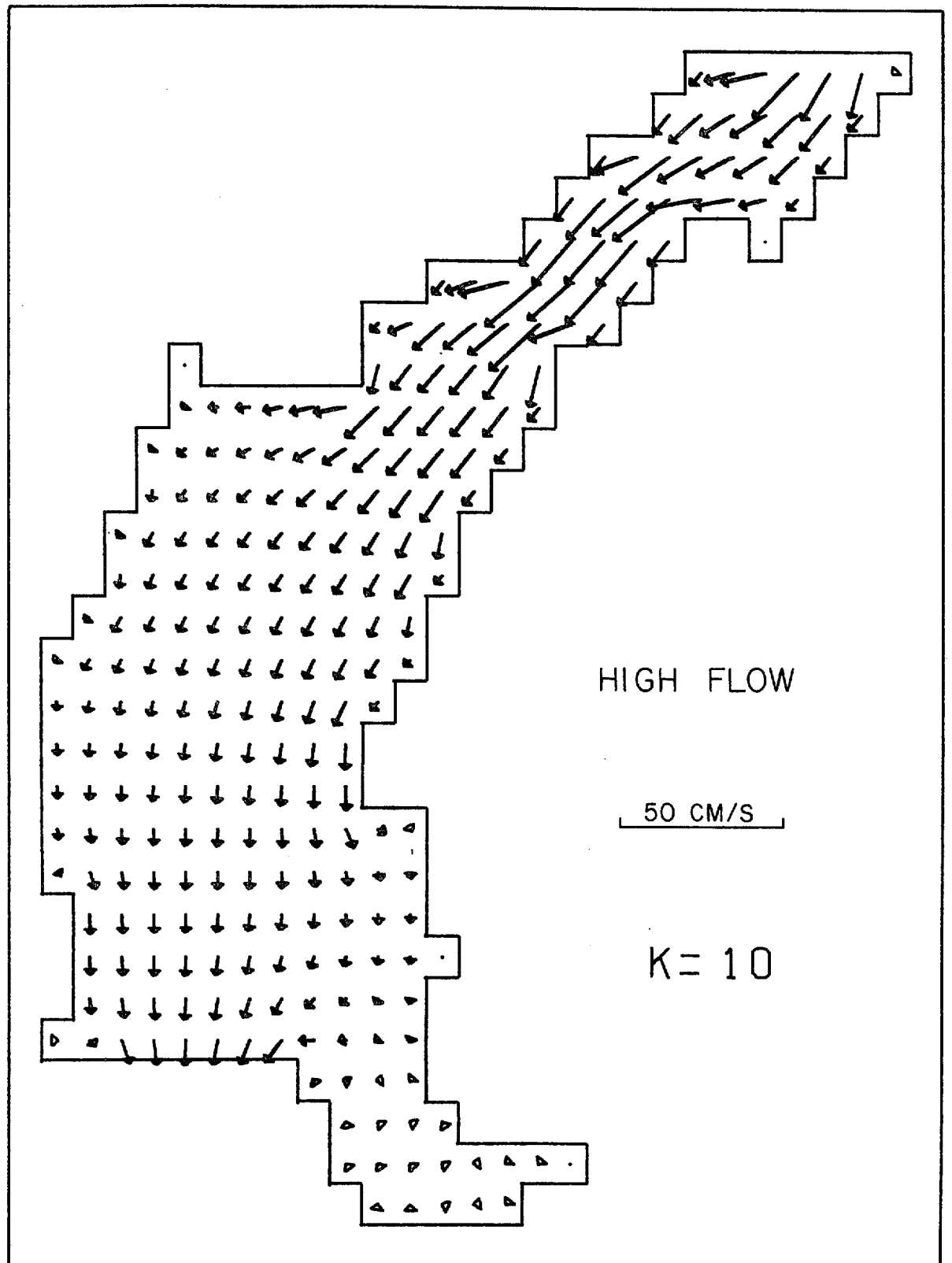
75151A410

Figure 10. Resultant Velocity Field for Level K = 10 Under High Flow Conditions
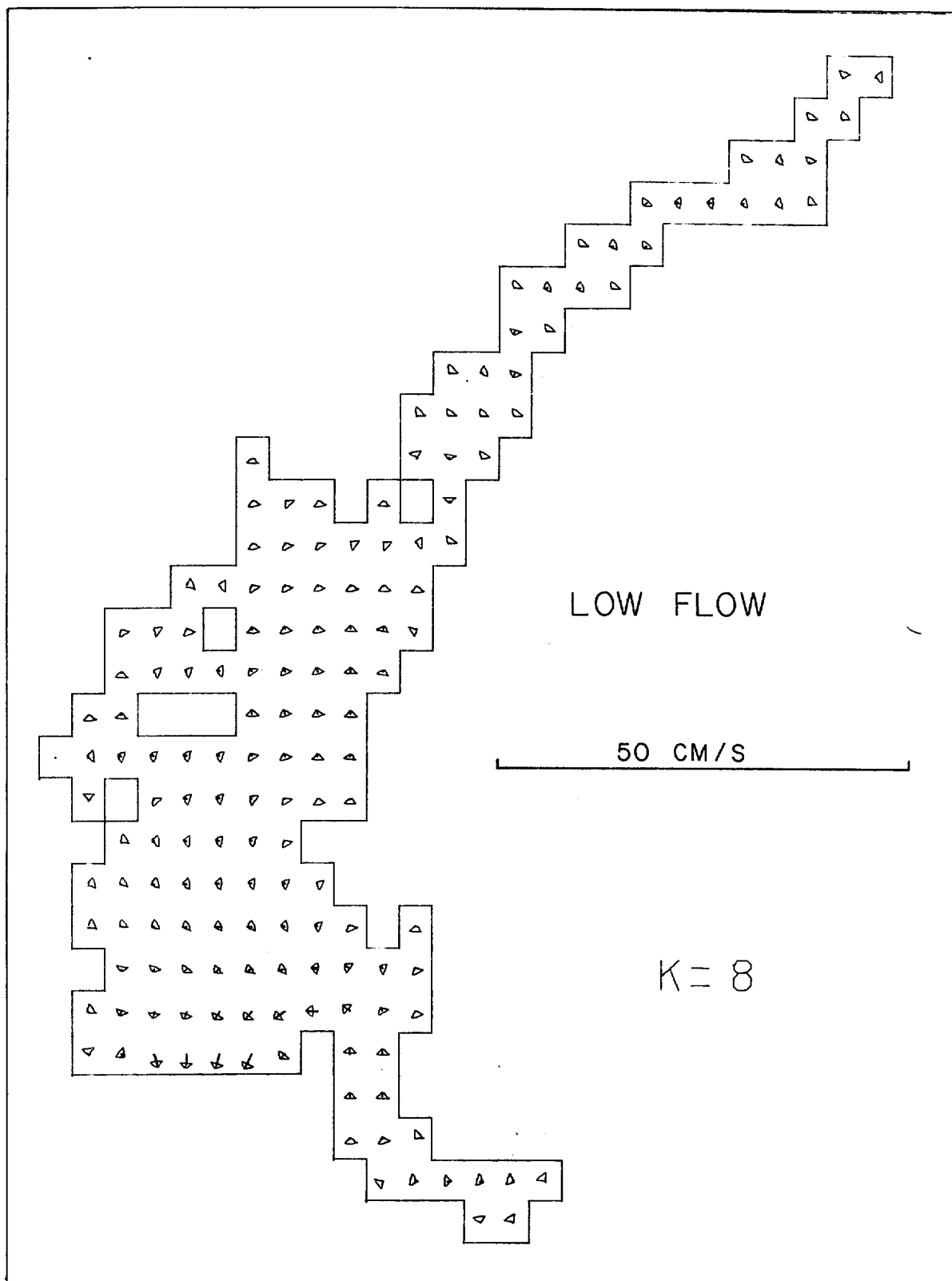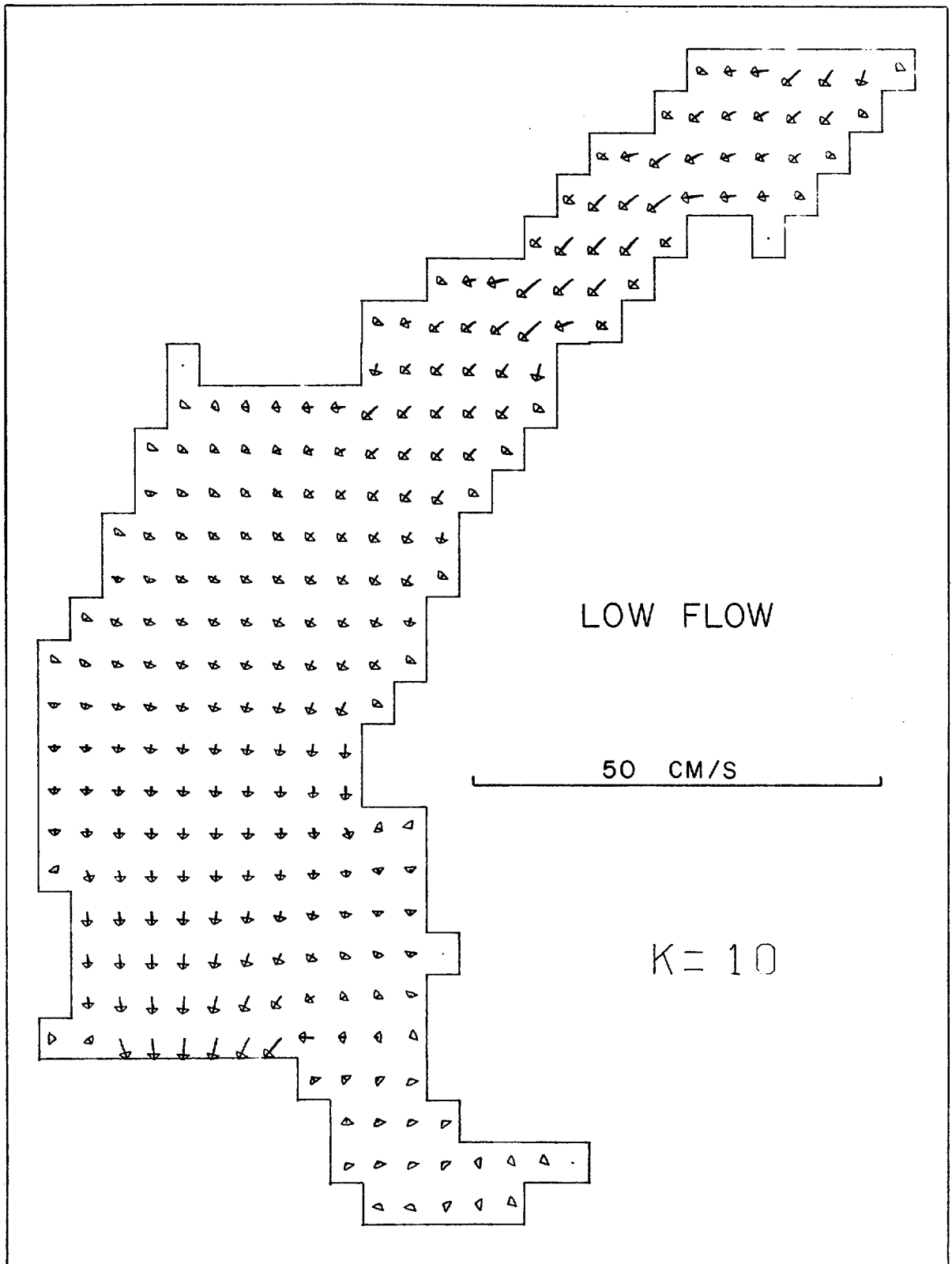
LOW FLOW

50 CM/S

K = 8

75151A411

Figure 11. Resultant Velocity Field for Level K = 8 Under Low Flow Conditions

LOW FLOW

50 CM/S

K = 10

Figure 12. Resultant Velocity Field for Level K = 10 Under Low Flow Conditions

The salinity data used were all the historic data stored in the Chesapeake Bay Institute data bank, excepting the six months following Tropical Storm Agnes (1972). The average of all the data within each box was assigned to that box point. No correction for tidal displacements was applied, introducing an rms error in position of ± 2.5 km. Interpolation to assign values to points where data did not exist was accomplished by the method described in Section 2.4.2. The data obtained unfortunately were very noisy, as shown by the surface salinities for the high and low flow periods in Figures 13 and 14.

The resultant exchange coefficients then were calculated by the method of Section 2.4 (Equation 29), using a gradient method of matrix inversion.

Primarily due to the poor salinity data used as input, the exchange coefficient data looked extremely noisy. The ratio of the standard deviation to the mean for each set of data (K_x, K_y, K_v) was in the order of one-twentieth.

The mean values of K_x, K_y, K_v were as follows (in cgs units):

|	K_x	K_y	K_v
High Flow	0.2125×10^6	0.2633×10^6	-14.48
Low Flow	0.09196×10^6	0.06806×10^6	5.705

These means were taken as follows:

K_x: mean taken over all x-facing faces
K_y: mean taken over all y-facing faces
K_v: mean taken over all z-facing faces except those adjacent to an open boundary, where it can be shown that the K_v values are incorrect.

The high flow values were rejected due to the negative value of K_v. Initially source predictions (Section 4.4) for the high flow and low flow suspended sediment data were carried out using the low flow exchange coefficients in both cases. Both the high flow and low flow source functions showed considerable noise, attributed primarily to an incorrect *vertical* exchange coefficient. Hence the least-squares method of determining the exchange coefficients (Section 2.5) was used, being applied to the *suspended sediment concentration data*. The following results were obtained (in cgs units):

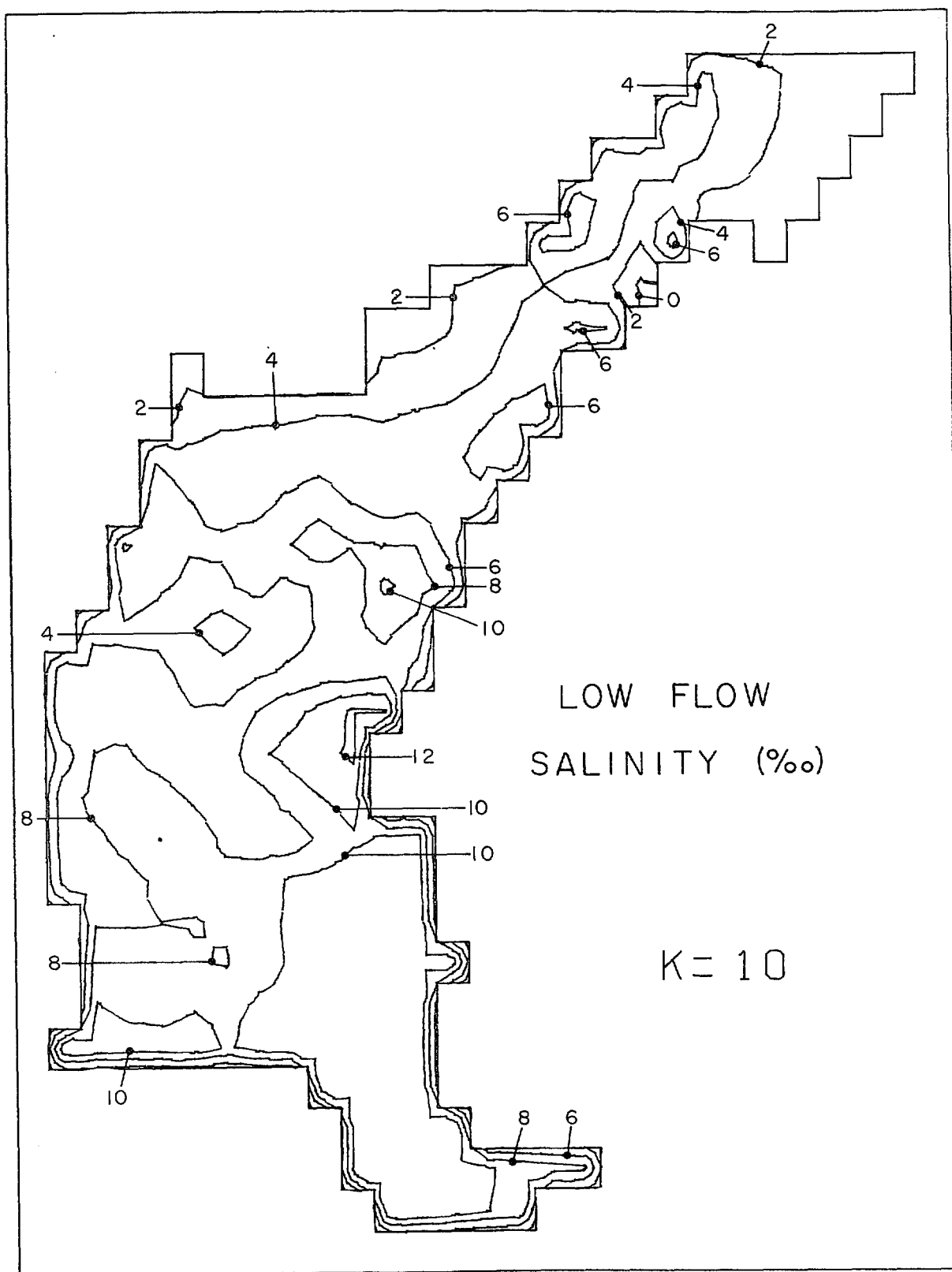|	K_H	K_v
High Flow	-0.1671×10^6	1.243
	0	1.244
Low Flow	-0.1065×10^6	0.3696
	0	0.4196

The negative value of K_H obtained as the first result for each season is unrealistic; hence, an additional constraint was applied:

$$K_H = 0.$$

HIGH FLOW

SALINITY (‰)

K = 10
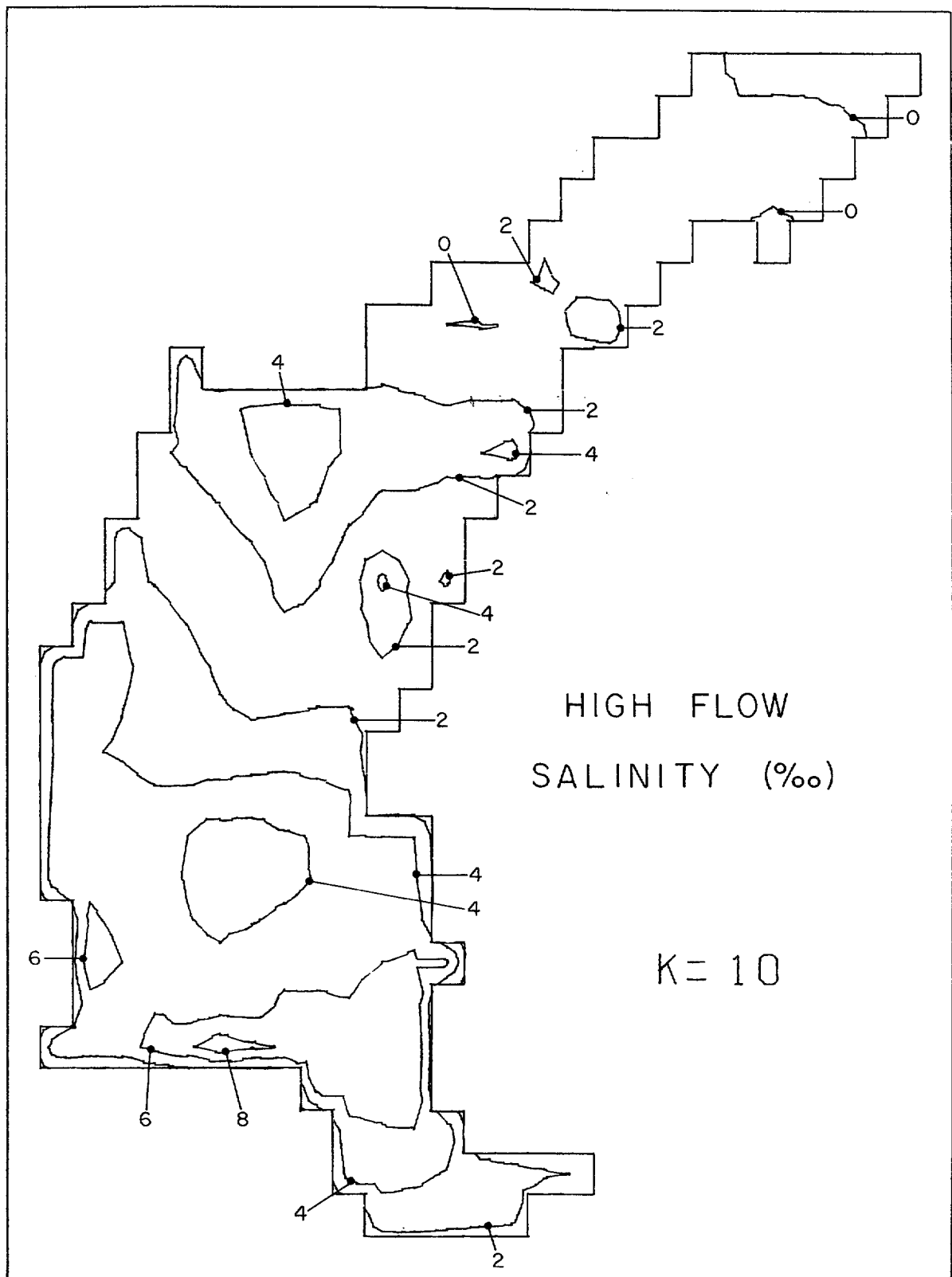
Figure 13. Surface Salinity, High Flow Condition

75151A413

LOW FLOW

SALINITY (‰)

K = 10

75151A414

Figure 14. Surface Salinity, Low Flow Condition

This yielded a slightly different optimum value of K_v (the second result for each season), but the resultant sums-of-squares values for the source function (SS of Section 2.5) was only marginally higher than in the case where K_H was allowed to be variable:

1.7 percent higher for the high flow season, and
3.8 percent higher for the low flow season.

Hence in the final evaluation of source functions the following exchange coefficients were used:

K_H = 0
K_v = 1.244 cgs (high flow) or
K_v = 0.4196 cgs (low flow).

The actual source sums-of-squares (SS of Section 2.5) were, in these cases:

High flow: 1.523×10^{-5} $(mg/\ell/sec)^2$
Low Flow: 4.824×10^{-7} $(mg/\ell/sec)^2$.

These sums-of-squares involved 324 values, and so the corresponding rms values were:

High flow: 2.17×10^{-4} $mg/\ell/sec$
Low flow: 3.86×10^{-5} $mg/\ell/sec$

Hence the resultant source fields have a noise associated with them when the rms values are as given above. As a rough guide, features of amplitude less than *twice* the rms values are probably artifacts of the modeling procedure and of errors in the data; hence they are not significant. Significant features are, therefore, those of amplifude greater than approximately:

High flow: 0.4×10^{-3} $mg/\ell/sec$
Low flow: 0.8×10^{-4} $mg/\ell/sec$.

4.4 Sediment and Contaminant Data

The model is intended as a predictor of PCB and CHC sources in the upper bay. These substances are known to be transported in association with suspended sediment particles, incorporated in planktonic organisms, and with the water. Because of the importance of transport on suspended sediment, and the absence of sufficient PCB and CHC data meeting the model requirements, the model was run on suspended sediment data only, of which there were:

High flow: 187 data points
Low flow: 232 data points.

The sediment data used in the model were from the following periods:

High flow: March 20 through 21, 1974
                April 16 and 25, 1974

Low flow: July 31 through August 1, 1974
                September 18 and 19, 1974
                October 7, 1974

Thus we solved for σ_1 only in Equation (6), Section 2. Multiplying this by a mean PCB concentration per unit mass of sediment would give the first term on the right-hand side of Equation (6). Thus, one can find *only* the sources of PCBs or CHCs *that are associated with sediment sources.*

The suspended sediment data were interpolated onto all the box points as in Section 4.2, where the method was applied to salinity. The resultant concentration fields are shown in Figures 15 through 18, for the high and low flow cases at depths K = 8 and K = 10.

4.5 Sediment Sources.

The sediment sources were calculated by a finite difference solution of Equation (2), Section 2 for the steady-state case. Ideally, as there can be no sediment sources in an isolated volume of water, the solution should give a zero source field for this case. A boundary condition of the model is that there is no flux of sediment through *any external boundary.* Hence, if there is a source of sediment on the bottom, the model will show a finite source at the box point adjacent to the bottom. Similarly at the point where the Susquehanna River enters the Chesapeake Bay, much sediment is advected through the boundary. This is shown in the model as a source of sediment at the box points adjacent to the boundary between the bay and the Susquehanna.

Thus, the proper interpretation of the source field given by the model is:

(1)   For a box point in the interior of the model but not adjacent to any external boundary, the source function should be zero. If it is not, then it indicates an error in the model prediction.

(2)   For a box point adjacent to an external boundary, a positive value of the source function represents an *inflow* of sediment through that boundary. Similarly a negative value represents an *outflow* of sediment through the boundary. If the box point is adjacent to the upper surface of the model only, then the source function should be zero, as the flux of sediment through the upper surface of the bay should be negligible. To convert from the source function units (mass of sediment/unit volume/unit time) to actual flux of sediment into a box, one must multiply by the box volume which is:

$$
\begin{aligned}
&(1'\ \text{latitude}) \times (1'\ \text{longitude}) \times (5\ \text{ft}) \\
=\ &185,400 \times 144,000 \times 152.4\ \text{cm}^3 \\
=\ &4.069 \times 10^{12}\text{cm}^3 = 4.069 \times 10^9\ \text{liters}.
\end{aligned}
$$

The source function units are mg/liter/sec; hence, multiplying by 4.069×10^9 gives flux units of mg/sec.

The vertical settling velocity for sediment was taken to be 10^{-3} cm/sec.

The source functions were first determined using exchange coefficients derived from the historical salinity data (Sections 2.4 and 4.3). The resultant source functions showed considerable noise, consisting mainly of combinations of *sources* and *sinks* (or negative *sources*) at different depths. This was most likely due to the use of an incorrect vertical exchange coefficient. As the sediment concentration in general *increases* with depth, an *over-large* vertical exchange coefficient will *increase* the vertical diffusive sediment flux and appear in the model as a *sink* near the surface and a *source* near the bottom. This was clearly the case in the central regions of the model in both the high and low flow cases. In the low flow case the results were so heavily contaminated with noise that no valid predictions could be made about the true source field.

As a result, the alternative method of exchange coefficient determination was used (Sections 2.5 and 4.3), and the resultant source field for high and low flow conditions and for depths K=6, K=7, K=8, K=9 and K=10 are shown in Figures 19 through 23 (high flow) and Figures 24 through 28 (low flow).

HIGH FLOW

SUSPENDED SEDIMENT

MG./LITRE

K= 8
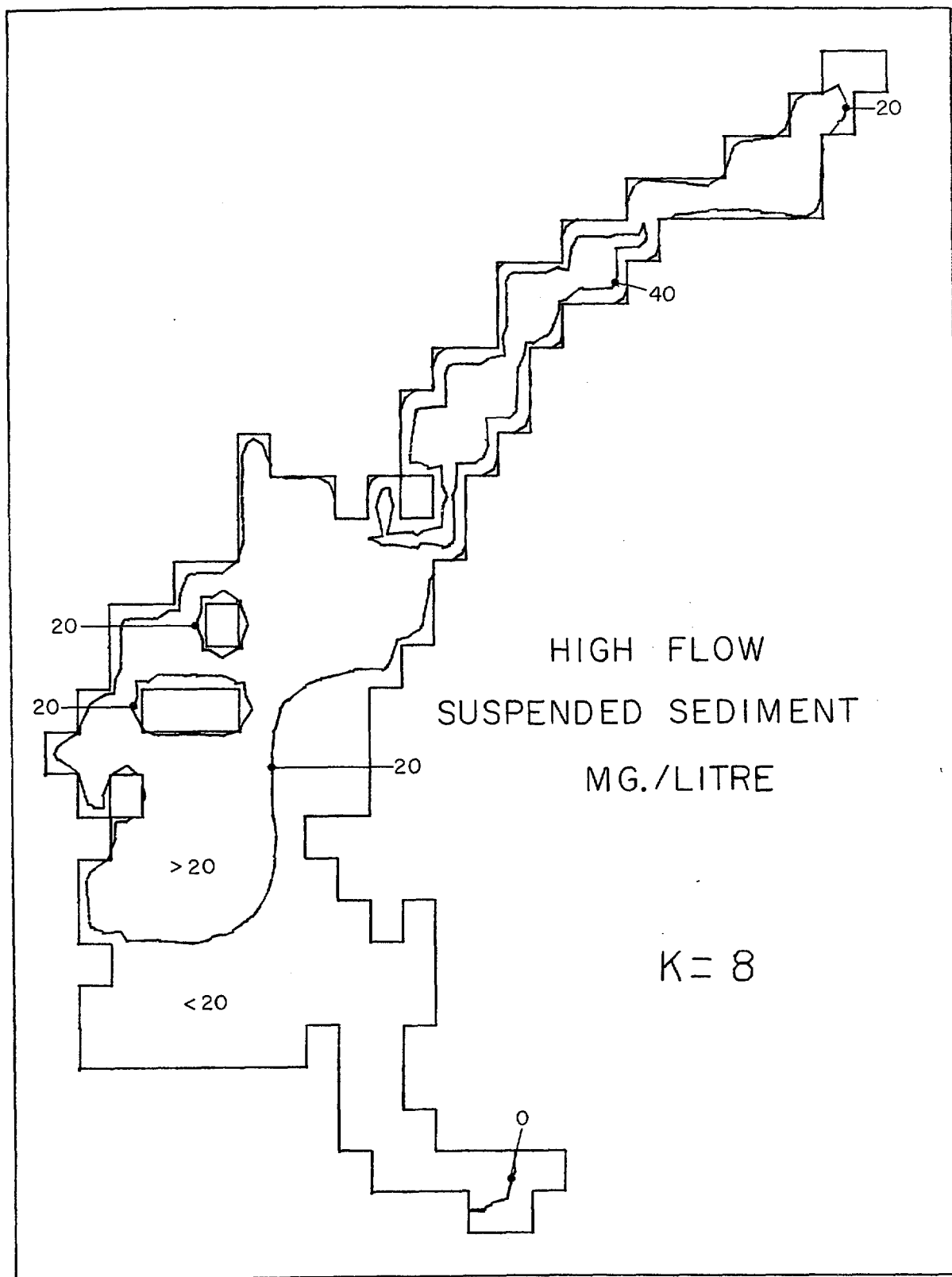
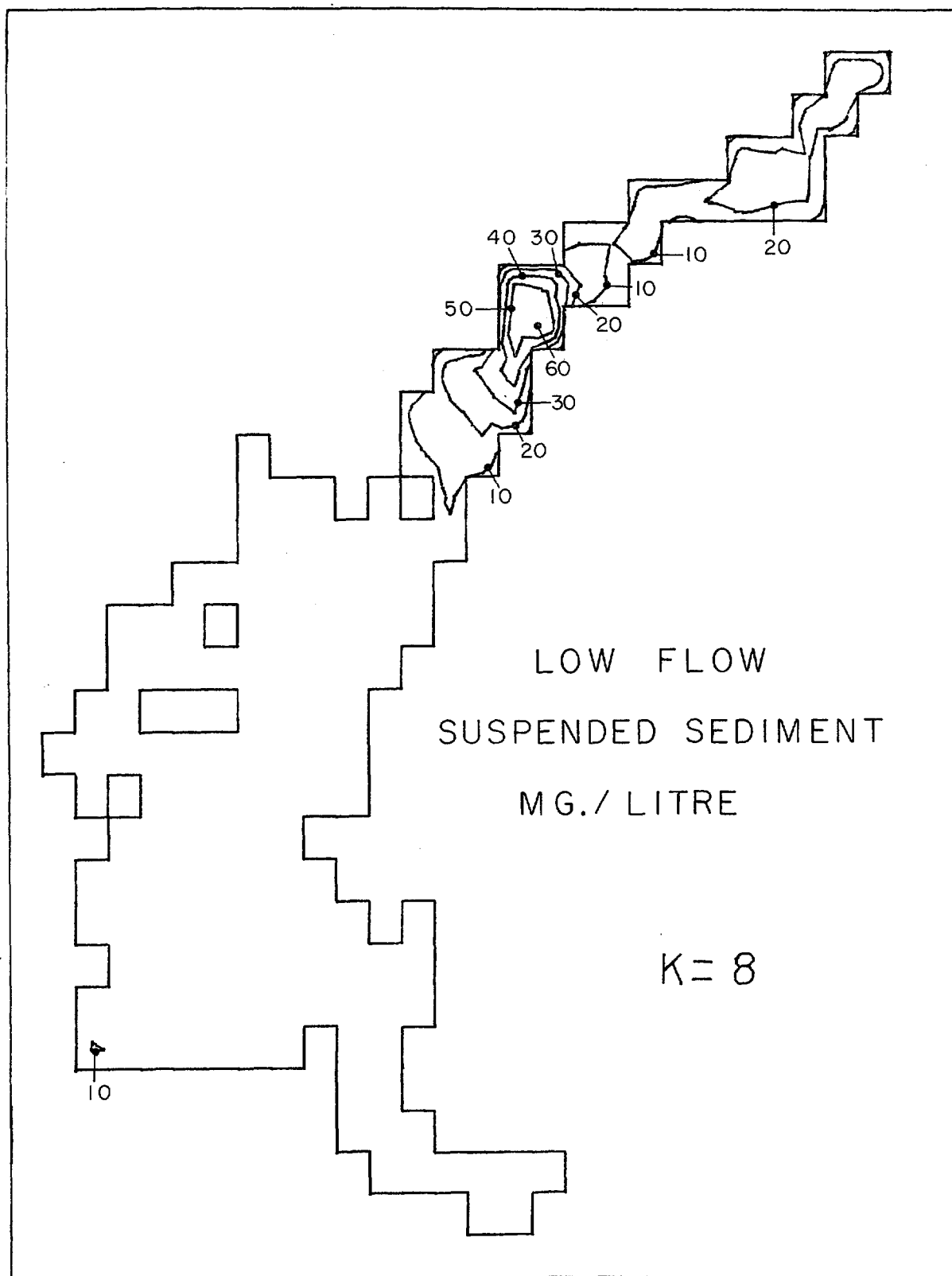Figure 15. Suspended Sediment Concentration Field at Depth K = 8
Under High Flow Conditions (Expressed in Milligrams per Liter)

HIGH FLOW

SUSPENDED SEDIMENT

MG./ LITRE

K = 10
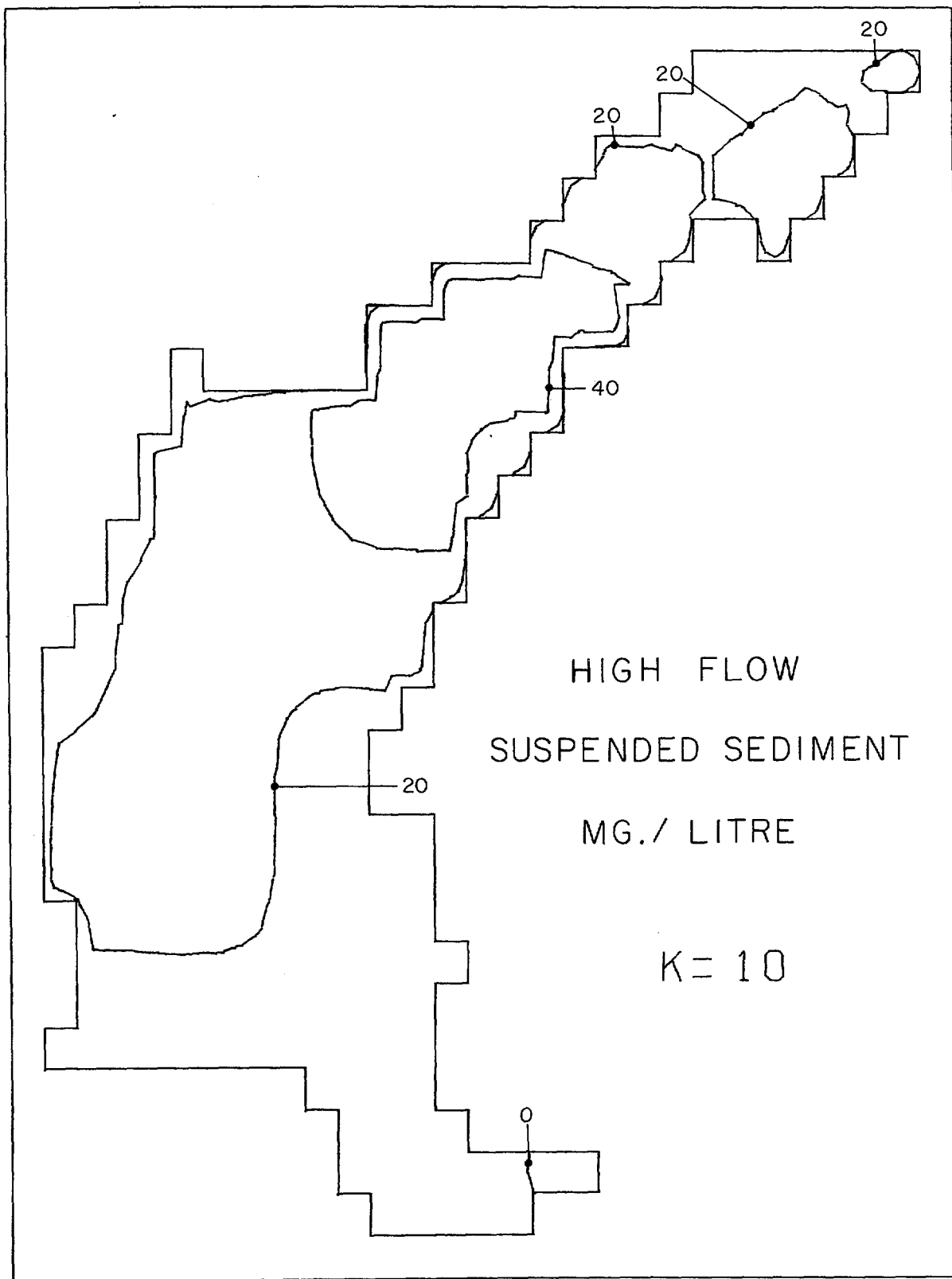
75151A416

Figure 16. Suspended Sediment Concentration Field at Depth K = 10
Under High Flow Conditions (Expressed in Milligrams per Liter)

LOW FLOW

SUSPENDED SEDIMENT

MG./LITRE

K = 8

75151A417

Figure 17. Suspended Sediment Concentration Field at Depth K = 8
Under Low Flow Conditions (Expressed in Milligrams per Liter)
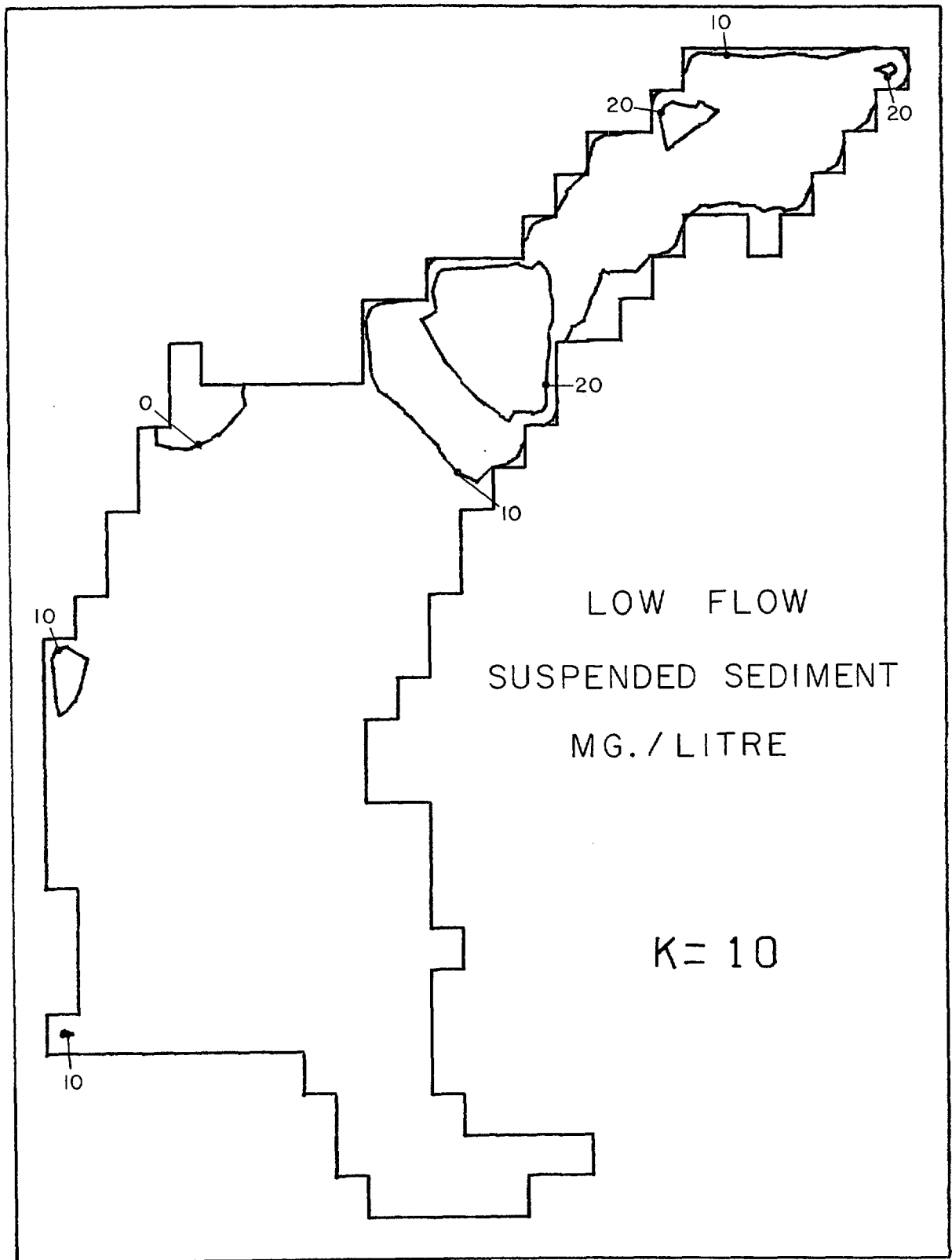
LOW FLOW

SUSPENDED SEDIMENT

MG./LITRE

K= 10

75151A418

Figure 18. Suspended Sediment Concentration Field at Depth K = 10
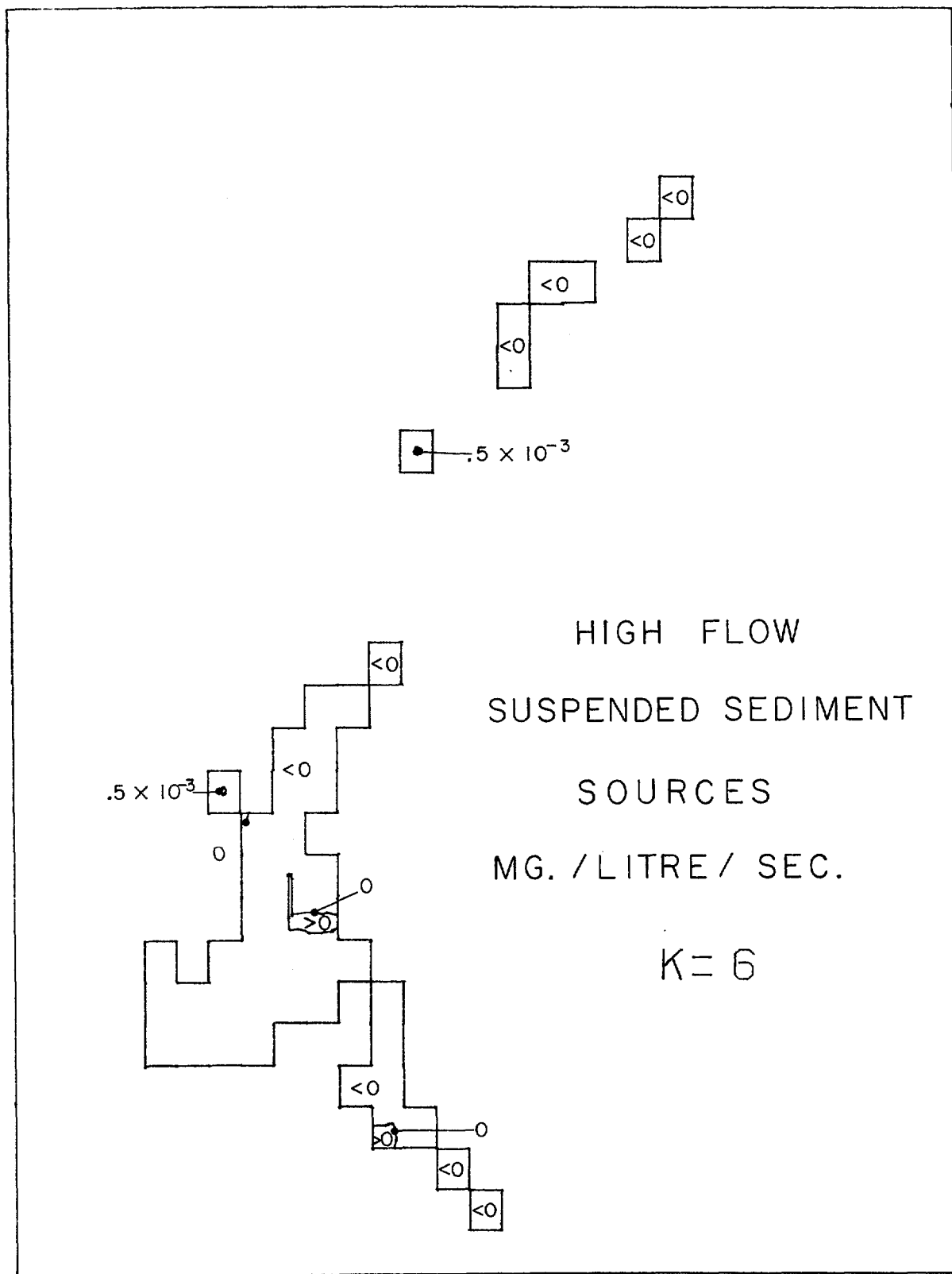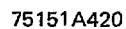*Under Low Flow Conditions (Expressed in Milligrams per Liter)*

4-18

HIGH FLOW

SUSPENDED SEDIMENT

SOURCES

MG. / LITRE / SEC.

$K = 6$

75151A419

*Figure 19. Suspended Sediment Source Field at Depth K = 6
Under High Flow Conditions*

Figure 20. Suspended Sediment Source Field at Depth K = 7
Under High Flow Conditions

75151A420

Figure 21. Suspended Sediment Source Field at Depth K = 8
Under High Flow Conditions

75151A421

7.9×10^{-3}

$-.5 \times 10^{-3}$

$-.5 \times 10^{-3}$

$.5 \times 10^{-3}$

$-.5 \times 10^{-3}$

$-.5 \times 10^{-3}$

$.5 \times 10^{-3}$

HIGH FLOW

SUSPENDED SEDIMENT
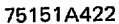
SOURCES

MG. / LITRE / SEC.

K = 9

$-.5 \times 10^{-3}$

75151A422

Figure 22. Suspended Sediment Source Field at Depth K = 9
Under High Flow Conditions

4-22

*Figure 23. Suspended Sediment Source Field at Depth K = 10
Under High Flow Conditions*

LOW FLOW

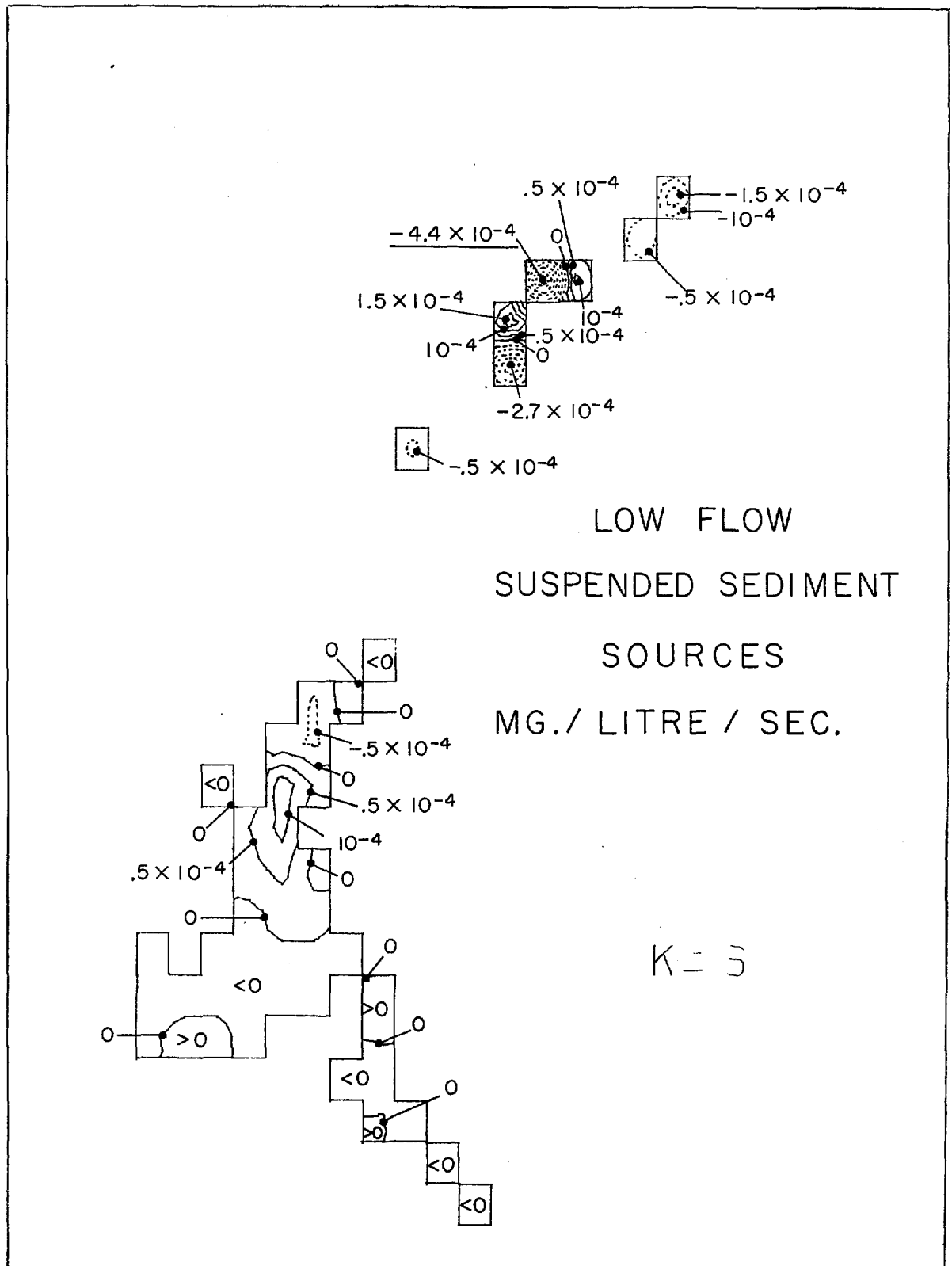**SUSPENDED SEDIMENT**

SOURCES

MG./ LITRE / SEC.

$K = 6$

75151A424

Figure 24. Suspended Sediment Source Field at Depth K = 6
Under Low Flow Conditions

Figure 25. Suspended Sediment Source Field at Depth K = 7
Under Low Flow Conditions

75151A425

LOW FLOW SUSPENDED SEDIMENT SOURCES MG./LITRE/SEC.

K = 8

75151A426

*Figure 26. Suspended Sediment Source Field at Depth K = 8
Under Low Flow Conditions*

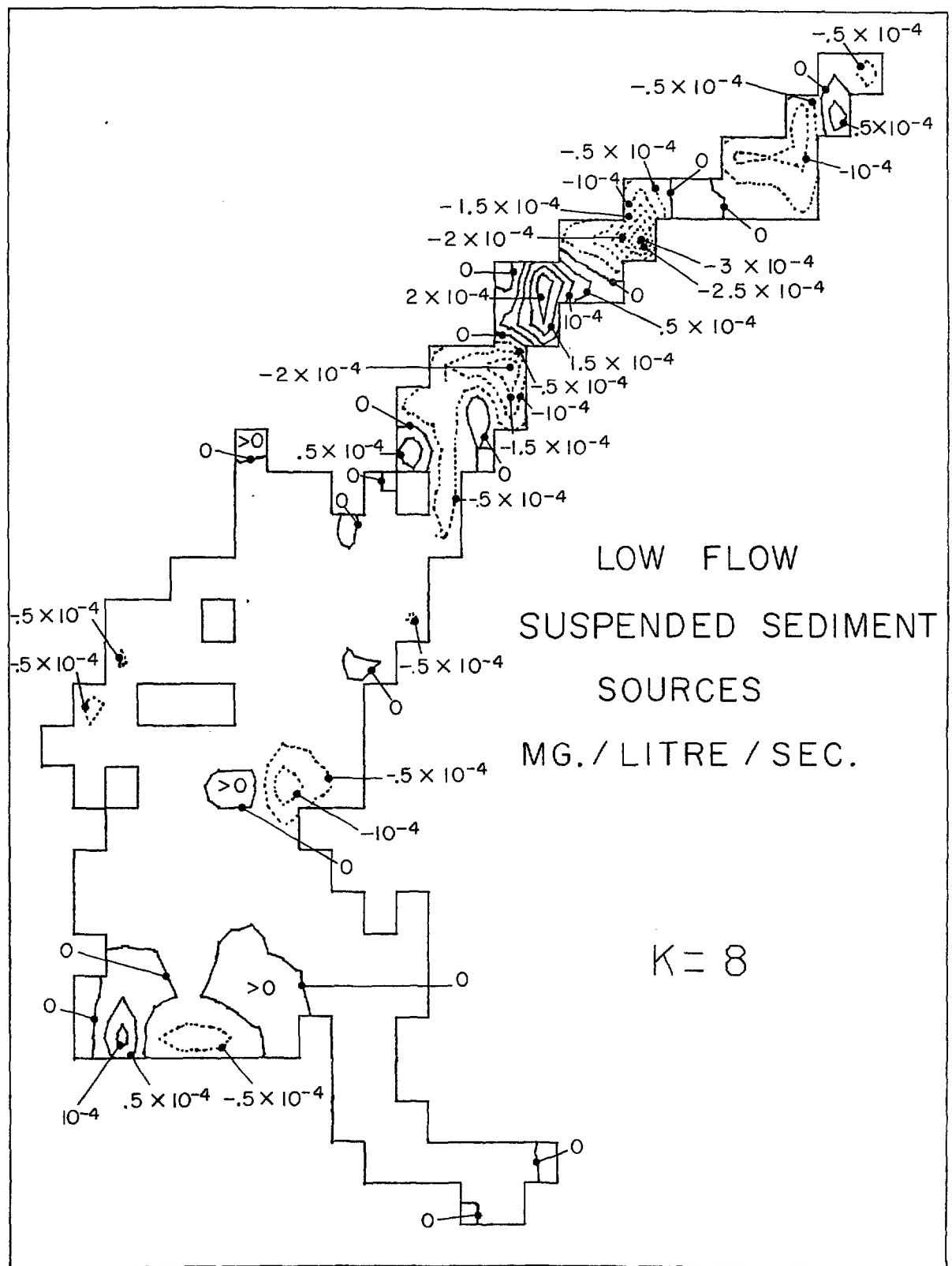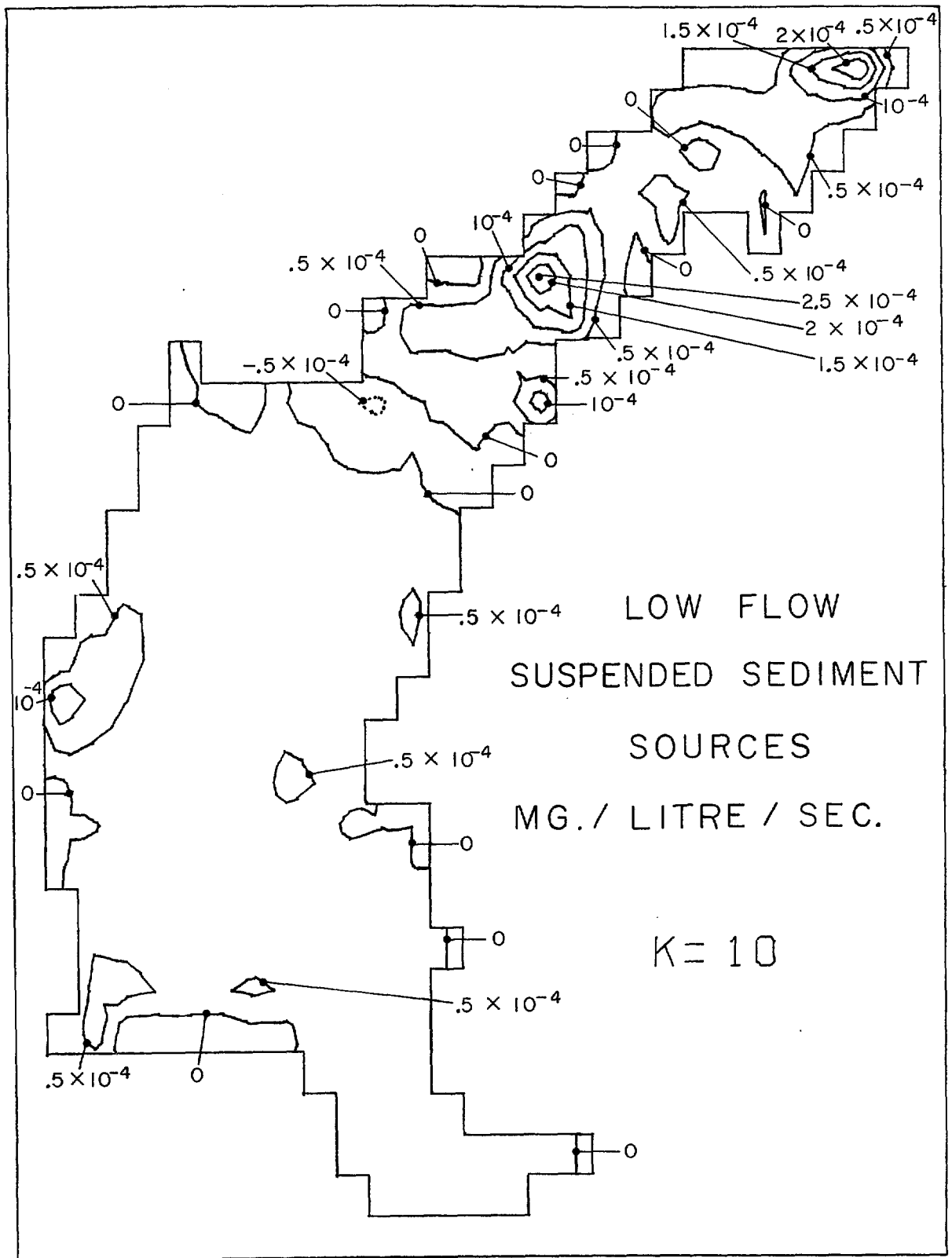LOW FLOW
SUSPENDED SEDIMENT
SOURCES
MG. / LITRE / SEC.

$K = 9$

75151A427

Figure 27. Suspended Sediment Source Field at Depth K = 9
Under Low Flow Conditions

Figure 28. Suspended Sediment Source Field at Depth K = 10
Under Low Flow Conditions

The significant features of these source fields are:

<u>High Flow Case:</u>

(1)   An input of sediment from the Susquehanna.
(2)   An output of sediment through the southern open boundary.
(3)   A source/sink combination associated with upper Chesapeake Bay Stations 5A and 5B.

The third is probably not a real feature but a combination of errors in the input data at these stations and an artifact of the modeling procedure. An important consideration is that when concentration data are fed into the model, it is assigned to the box point nearest to the points at which the data were taken. Thus a position of error of $\pm \sqrt{\delta x^2 + \delta y^2}/2$ at most is introduced. This becomes important where there are high horizontal gradients in the suspended sediment concentration.

<u>Low Flow Case:</u>

(1)   An input of sediment from the Susquehanna River.
(2)   An output of sediment through the southern open boundary.
(3)   A source/sink combination associated with upper Chesapeake Bay Stations 4A, 4B, and 4C. (Again, this is probably not real as in the high flow case above.)
(4)   A source/sink combination associated with the region between upper Chesapeake Bay Sections 4 and 5. (Again, this is probably not real as in the high flow case above.)
(5)   A source/sink combination associated with a station designated 922Y in the Chesapeake Bay Institute data bank. (Again this is probably not real as in the high flow case above.)

These results do not look very promising as they do not reveal any more than was known already—that sediment enters the bay via the Susquehanna River and leaves it by the southern open boundary. It is easy to see why this is so if one looks at the orders of magnitude of the various sources.

The flows of suspended sediment from the Susquehanna River and through the southern open boundary are roughly:

	High Flow	Low Flow
Susquehanna	60×10^6 mg/sec	7×10^6 mg/sec
Southern boundary	30×10^6 mg/sec	2×10^6 mg/sec
Difference	30×10^6 mg/sec	5×10^6 mg/sec

If the differences were accounted for by a uniform deposition over the whole of the upper bay, these would appear as sources of the following magnitude in the bottom boxes of the model:

High Flow: -3×10^{-5} mg/ℓ/sec
Low Flow: -5×10^{-6} mg/ℓ/sec

Comparing these with the amplitudes of significant features given in Section 4.3, it is seen that:

$$\frac{\text{source at bottom due to sedimentation}}{\text{amplitude of significant features}} \sim \frac{1}{15} ;$$

hence, such real sources would be well below the noise level. Sedimentation would only be apparent as a real feature in the resultant source fields if *all* the accumulation of sediment in the upper bay were concentrated in less than one-fifteenth of the total area of the bottom.

In order to remove some of the noise in the predicted sources, *vertical integration* from the bottom to the surface was carried out on the source fields. Cancellation of the vertical sediment fluxes rendered the results independent of vertical advection velocity, vertical settling velocity, and vertical exchange coefficient. Because the horizontal exchange coefficient was taken as zero, the resultant source fields are due to a *three-dimensional model* in which *horizontal* exchange is by *advection only - -there is no constraint whatsoever on vertical exchange.*

The source fields given now represent the source of sediment *per unit horizontal area.* A flux of sediment through a vertical boundary is represented as a source or sink in the box adjacent to that boundary. To convert this source (mass of sediment/unit area/unit time) to an actual flux of sediment one must multiply by the *box area* which is:

$$\begin{aligned} &(1' \text{ latitude}) \times (1' \text{ longitude}) \\ = \ &185{,}400 \times 144{,}000 \text{ cm}^2 \\ = \ &2.700 \times 10^{10} \text{ cm}^2 \end{aligned}$$

The source function units are micrograms per square centimeter per second ($\mu g/cm^2/sec$); hence, multiplying by 2.700×10^{10} cm^2 gives flux units of $\mu g/sec$.

The results are shown in Figures 29 and 30 for high flow and low flow cases respectively. For clarity, positive values of the source function are shown by shaded areas. These results look very much less noisy than the source fields before integration, and they probably represent *the best estimates of sources and sinks in the upper Chesapeake Bay generated so far by the model.*

Again fluxes of sediment through the northern and southern open boundaries are evident. The variations in source field across the southern boundary in the low flow case may be due to errors in the input data in this region or an artifact of the model. An interesting, and probably real feature of the source fields- -especially in the southern and middle areas of the model- -is the way in which many regions are shown as a source in one season and a partially compensating sink in the other. Thus, the source field shows a strong variation from season to season, many regions alternating between sedimentation and resuspension during the year.

Note that some regions of the model have little or no suspended sediment data; hence, the predicted source fields in these regions are a function of the interpolation procedures used rather than of any real phenomena. Such regions are:
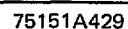
(1)   The Chester River
(2)   The mouths of the Gunpowder, Middle, and Back Rivers

4.6 Conclusions

It must be emphasized that the vertically integrated sediment source fields derived here are only tentative. They are a function of the velocity field, the suspended sediment concentration field, and the interpolation procedure used to derive it, as well as the fact that horizontal diffusive exchange is neglected. Ideally, investigations should be carried out as to the sensitivity of the predicted source field to these input parameters and to the factors upon which they depend.
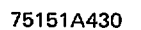
Based on the availability of current velocity and suspended sediment data at the present time, it would appear that the most reasonable predictions of suspended sediment sources can be obtained by the following combinations of models:

(1)   A pseudo-dynamic model (Section 2.3) or, better, a full dynamic model (which does not at present exist) of the velocity field in three dimensions.

(2)   A prediction model for the *vertically integrated source field* of suspended sediment, based initially on a zero horizontal exchange coefficient and later on a finite one, if it appears necessary.

Figure 29. Vertically Integrated Suspended Sediment Source
Field Under High Flow Conditions

75151A429

Figure 30. *Vertically Integrated Suspended Sediment Source Field Under Low Flow Conditions*

75151A430

Data requirements for one run of the model are:
(1) The discharge of the Susquehanna River at Conowingo.
(2) Current meter records at the southern open boundary of the model [roughly three moorings with three meters per mooring—these data to be used as the boundary condition for the pseudo-dynamic model (Section 2.3)]. Current meter records are also required from stations in the interior of the model [roughly three moorings with three meters per mooring—these data to be used as a means of choosing the optimum value of K in the pseudo-dynamic model, using Equation (27)]. The duration of these records should be at least 30 days, and the recording interval should be 30 minutes or less.
(3) Vertical profiles of the suspended sediment concentration (and, if applicable, the concentration of sediment-borne contaminant) at roughly 30 stations in the upper Chesapeake Bay.

4.7 References

Boicourt, W. C., 1969. A Numerical Model of the Salinity Distribution in Upper Chesapeake Bay. Chesapeake Bay Institute, The Johns Hopkins University, Technical Report 54, Ref. 69-7.

Caponi, E. A., 1974. A Three-Dimensional Model for the Numerical Simulation of Estuaries. University of Maryland, Institute for Fluid Dynamics and Applied Mechanics, Technical Note BN-800.

Cartwright, D. E., . . ., N.I.O. Program 158. Institute of Oceanographic Sciences, Wormley, England.

Feister, C. and Karweit, M., 1973. Data Bank Inventory, Vol II, Chesapeake Bay, Edition 1, 1949 through 1970. Chesapeake Bay Institute, The Johns Hopkins University, Data Bank Report 2, Ref. 73-5.

Klepper, J. C., 1972. A Report on the Prototype Current Velocity and Salinity Data Collected in the Upper Chesapeake Bay for the Chesapeake Bay Model Study. Chesapeake Bay Institute, The Johns Hopkins University, Special Report 27, Ref. 72-12.

Leendertse, J. J., Alexander, R. C., and Liu, S., 1973. A Three-Dimensional Model for Estuaries and Coastal Seas: Volume 1, Principles of Computation. The Rand Corporation, R-1417-OWRR.

Pritchard, D. W., 1958. The Equations of Mass Continuity and Salt Continuity in Estuaries. Journal of Marine Research. Vol. 17, pp. 412-423.

Seitz, R. C., 1971. Drainage Area Statistics for the Chesapeake Bay Fresh-water Drainage Basin. Chesapeake Bay Institute, The Johns Hopkins University, Special Report 19, Ref. 71-1.